NOVA SCHOOL OF SCIENCE & TECHNOLOGY

DEPARTAMENT OF LIFE SCIENCES

GUILHERME DAVID CASTRO MARTINS

BSc in Biochemistry

# UNVEILING THE ROLE OF DPS, ENDOIII AND PPK FOR DNA PROTECTION AND REPAIR IN *DEINOCOCCUS RADIODURANS* UPON EXPOSURE TO GENOTOXIC STRESS

MASTER IN MOLECULAR GENETICS AND BIOMEDICINE

NOVA University Lisbon

September, 2022

NOVA SCHOOL OF SCIENCE & TECHNOLOGY

DEPARTMENT OF LIFE SCIENCES

# UNVEILING THE ROLE OF DPS, ENDOIII AND PPK FOR DNA PROTECTION AND REPAIR IN *DEINOCOCCUS RADIODURANS* UPON EXPOSURE TO GENOTOXIC STRESS

**GUILHERME DAVID CASTRO MARTINS**

BSc in Biochemistry

**Advisers:** Célia Romão
*Researcher, ITQB-NOVA, UNL*

**Co-adviser:** Sérgio Filipe
*Auxiliar Professor, FCT-NOVA, UNL*

**Examination Committee:**

**Chair:** Paula Gonçalves
*Associated Professor, FCT-NOVA, UNL*

**Rapporteurs:** Ana Margarida Saramago
*Post-Doc Researcher, ITQB-NOVA, UNL*

**Adviser:** Célia Romão
*Researcher, ITQB-NOVA, UNL*

MASTER IN MOLECULAR GENETICS AND BIOMEDICINE

NOVA University Lisbon
September, 2022

**UNVEILING THE ROLE OF DPS, ENDOIII AND PPK FOR DNA PROTECTION AND REPAIR IN *DEINOCOCCUS RADIODURANS* UPON EXPOSURE TO GENOTOXIC STRESS**

# ACKNOWLEDGMENTS

Firstly, I would really like to thank both my principal supervisors, Célia Romão and Elin Moe, for everything that happened throughout this year. Thank you for being so supportive and for always believing in me. I have no words for what you did for me. Besides all this, you have provided me with great experiences regarding the divulgation of my work that I will never forget. Everything and anything that I reach and do from now on is thanks to you. I would also like to thank my co-supervisor, Professor Sérgio Filipe, for giving feedback on my experimental work.

I would like to thank FCT-UNL and ITQB-NOVA for allowing me to deepen my knowledge and for always providing the conditions for the development of my experimental work.

I can´t thank André Gouveia enough for what he has done for me. Since the start that he has been such an amazing person and has taught me so and so much. His loud and warm "Bom dia" each and every morning really had an effect and made the laboratorial work seem lighter. He is a really great scientist, really passionate with his work, and I am really proud of him and the work he has been doing! I will never forget the things you did for me.

I have to thank the Macromolecular Crystallography Unit, as well, for receiving me into their team and the environment always being great to work in. In particular, Filipe Rollo, Bruno Salgueiro, Carlota Conceição, and Dalila Fernandes for always helping me with anything I needed. Besides the unit, I would also like to thank João Carita for helping me in crucial steps of my experimental work and Catarina Paquete for giving me an excellent idea to solve one big problem I was having during the experimental work. Another person which had a really great impact in the last stage of my thesis was professora Helena Santos for allowing me to participate and present my work in the 2022 extremophiles meeting. Thank you so much. I will never forget that incredible experience.

Now, moving on to the personal side, all of this is thanks to my parents, who allowed me to keep studying and were always friends of mine and only wanted the best for me. I want to thank my brother and my sister-in-law for giving me a laptop when I desperately needed one. This is for you Ricardo and Catarina.

I thank deeply to my girlfriend, Inês Cebola, who was there, right by my side, in the good and in the bad moments throughout this year. She was a really important person in this process, whether it was cheering for a great result or thinking about what was going wrong with the experiment. Without whom I would not be able to keep on working in the bad days. Thank you so much for being so supportive and present in everything. And for helping me so much even though you had to work in your own thesis as well.

I really want to thank my close group of friends, ChL, which despite not being directly involved in my thesis made this entire process much easier. I can not explain how much they were important.

Without all this people, this thesis would not have been the same, so I owe it all to you! Thank you so much for everything.

# ABSTRACT

*Deinococcus radiodurans* (*Dr*) is known for showing great resistance to ionizing radiation, and desiccation amongst other extreme conditions. This bacterium possesses different groups of proteins which are involved in the response to several stress agents by either protecting the DNA from suffering damage, repairing efficiently the damaged DNA or even being involved in the metabolism small antioxidant molecules, capable of protecting the proteome so that it can continue working under stress conditions. In this work we focused on two DNA binding protein under starved conditions (Dps1 and Dps2) present in *Dr*, which are able to bind and protect DNA against damage, on three Endonuclease III proteins (EndoIII-1, EndoIII-2 and EndoIII-3) which remove oxidation damaged bases in DNA through the Base Excision Repair (BER) pathway and on two Polyphosphate kinases (PPK1 and PPK2) that are responsible for the metabolism of inorganic polyphosphate (PolyP) which is involved in the defense against oxidative stress. To understand the role of these proteins and their possible interplay, we constructed and studied the resistance to stress of both single, double and triple knockout mutants, of each of these proteins, through the Tripartite Ligation Method, using Overlap PCR. The induced stress was exposure to UV-C radiation, hydrogen peroxide and methyl viologen. The stress response was compared with the wild type bacterium. Moreover, a single amino acid mutation of EndoIII-2 was generated in order to attempt its crystallization, to understand its structure and the molecular mechanisms involved in its activity.

**Keywords**: *Deinococcus radiodurans*, DNA repair, DNA protection, Oxidative stress, Ultraviolet radiation

# RESUMO

*Deinococcus radiodurans* (*Dr*) é uma bactéria conhecida por demonstrar uma extraordinária resistência a radiação ionizante, desidratação extrema, stress oxidativo entre outras condições extremas. Esta bactéria possui diferentes famílias de proteínas que estão envolvidas na resposta a diferentes agentes de stress quer através de proteger diretamente o DNA, reparar eficientemente o DNA danificado ou ainda através de estarem envolvidas no metabolismo de moléculas antioxidantes de pequenas dimensões que estão envolvidos na proteção do proteoma em caso de dano severo. Este trabalho focou-se em 2 Dps (DNA binding protein under starved conditions) presentes em *Dr* (Dps1 e Dps2), que se ligam ao DNA protegendo-o de dano, em 3 Endonucleases III (EndoIII-1, EndoIII-2 e EndoIII-3) que são responsáveis por reparar o DNA danificado através do mecanismo de reparação por excisão de base e ainda em 2 cinases polifosfatases (PPK1 e PPK2) que são responsáveis pelo metabolismo de polifosfato inorgânico que está envolvido na defesa contra stress oxidativo. Com o intuito de compreender o papel de cada uma destas proteínas e estudar uma possível cooperação entre elas, foram construídos mutantes de deleção simples, duplos e triplos, através do método de ligação tripartido, usando PCR de fusão. O stress induzido foi a exposição a radiação ultravioleta-C, peróxido de hidrogénio e metil viologénio e a resposta a estas condições foi comparada com a resposta obtida pela bactéria nativa. Adicionalmente, uma alteração de um aminoácido na sequência da EndoIII-2 foi construída de maneira a tentar proceder à sua cristalização de maneira a compreender a sua estrutura e os mecanismos moleculares envolvidos na sua atividade.

**Palavras-chave:** *Deinococcus radiodurans*, reparação de ADN, proteção de ADN, stress oxidativo, radiação ultravioleta.

# ABBREVIATIONS

| | |
|---|---|
| **APS** | Ammonium persulfate |
| **Bp** | Base pair |
| **CAM** | Chloramphenicol Resistance Gene |
| **CFU** | Colony forming units |
| **Da** | Dalton |
| **dd$H_2O$** | Bidistilled water |
| **DMSO** | Dimethyl sulfoxide |
| **DNA** | Desoxyribonucleic acid |
| **dNTP** | Deoxyribonucleotide |
| ***Dr*** | Deinococcus radiodurans |
| **DSB** | Double strand break |
| **Dps** | Damage under starvation |
| **EDTA** | Ethylenediaminetetraacetic acid |
| **EndoIII** | EndonucleaseIII |
| **gDNA** | Genomic DNA |
| **Gy** | Gray |
| **Hygro** | Hygromycin Resistance Gene |
| **IPTG** | Isopropyl $\beta$ -d-1-thiogalactopyranoside |
| **Kb** | Kilo base |

| | |
|---|---|
| **LB** | Luria Bertani |
| **MW** | Molecular weight |
| **OD** | Optical density |
| **PCR** | Polymerase Chain Reaction |
| **pDNA** | Plasmid DNA |
| **PPK** | Polyphosphate kinase |
| **ROS** | Reactive oxygen species |
| **SDS** | Sodium Dodecyl Sulfate |
| **ssDNA** | Single strand DNA |
| **SOC** | Super Optimal broth with Catabolite repression |
| **TAE** | Tris-acetate-EDTA |
| **TEMED** | Tetramethylethylenediamine |
| **UV** | Ultraviolet |
| **WT** | Wild Type |

# CONTENTS

# LIST OF FIGURES

# LIST OF TABLES

# 1

# INTRODUCTION

## 1.1 *Deinococcus radiodurans*

The *Deinococcus* genus is composed of more than 50 radiation resistant species[2]. The origin of the name is from the Greek language in which "deinos" means "strange" and "coccus" reveals their granule shape structure. Most of these species organize as tetrads in liquid culture and are pigmented due the presence of a carotenoid pigment named deinoxanthin, that has been associated with the resistance to extreme conditions acquired by these microorganisms[3], as will be discussed further ahead.

*Deinococcus radiodurans* (*Dr*) was the first species of this genus to be isolated and it is known for its extraordinary radiation resistance and great endurance to desiccation and other extreme conditions[4,5]. This resistance has been attributed to several factors, from the highly efficient repair and protection enzymatic systems, other non-enzymatic pathways and even the toroidal structure of DNA observed in *Dr* cells[6]. It was the first species of this genus with the entire genome sequenced and annotated[7]. Because of this, *Dr* has been the focus of several studies, and it is a great model organism to study DNA damage and repair and the response against oxidative stress and radiation.

*Dr* was firstly identified as a contaminant from irradiated canned meat[7,8]. Their natural habitat is not defined yet as the species from this genus have been isolated from different areas of the planet, organic nutrients rich environments, animal feces, sewage, dried foods, medical instruments and even room dust[9]. *Dr* is a pink pigmented, spherical bacterium that has 1.5 to 3.5μM in diameter[9]. It is characterized as a gram-positive bacterium, as it presents a thick peptidoglycan layer, but has a similar cell envelope to gram negative bacteria[5,9]. This characteristic has been associated with its extraordinary resistance as, in general, it has been

observed that the more resistant organisms are gram-positive while the most sensitive organisms are gram-negative[10,11]. Its optimal growth temperature is 30ºC in rich medium and it an obligate aerobe[12].

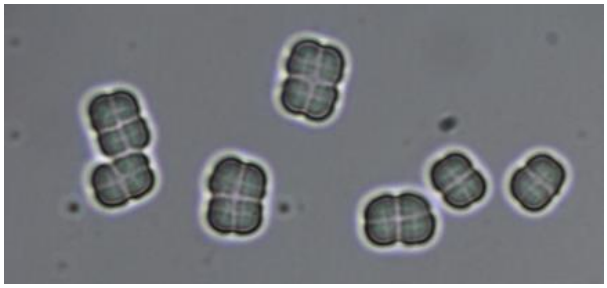

Figure 1.1 Visualization of *Deinococcus radiodurans*, of optical microscopy, in M53.

The *Dr* chromosome has 3.28 Mega base pairs (Mb), with a GC content of 66.6%. The genome is segmented and consists of a 2.64 Mb chromosome (chromosome I), a 0.41 Mb chromosome (chromosome II), a 0.18 Mb mega plasmid and a 0.045 Mb plasmid[7]. *Dr* has between 4 and 10 genome copies per cell, depending on the stage of the bacterial growth phase. This genome redundancy has been proposed to, in conjunction with the other defense mechanisms, play a role in the endurance of a microorganism against extreme damage to the DNA has it allows the cells to have multiple copies of each gene, reassuring the activity of a specific protein in the case of damage to a copy of an essential gene, as shown in [13].

Radiation is one of the most hazardous conditions in the environment which lead to the loss of viability, in cases of extreme doses, of radiation sensitive organisms. Two types of radiation that have been linked with causing DNA damage are Ultraviolet and gamma (γ)[14]. The ability of *Dr* of withstand high doses of these types of radiation is what classifies it as an extremophile as a radiation resistant organism. This bacterium shows no loss of viability after exposure to doses up to 5 kGray (kGy) of γ radiation[15], whereas less than 500 Gy causes the death of most other bacteria, like *E. coli* [9]. This does not mean that the DNA of *Dr* does not suffer any damage. In fact, 5kGy of γ radiation causes extreme amounts of double strand breaks (DSB's), forming hundreds of DNA fragments[16].

Initial studies suggested that DNA was the main target of damage during exposure to radiation, being the cause for loss of viability[17,18]. It was also proposed that the genome of *Dr* was protected from this damage allowing the cells to survive in these extreme conditions. Later it was found that the genome of *Dr* suffered approximately the same amount of DSB's as other radiation susceptible organisms[18]. Based on these results, new hypotheses were

proposed for the resistance of *Dr*. Currently, an efficient proteome protection against reactive oxygen species (ROS)-induced stress and a better ROS scavenging system is proposed to be the main difference between radiation resistant and susceptible species[17].

In *Dr* it has been proposed[19] that low molecular weight manganese complexes are involved in the scavenging of ROS, and possibly even helping in the recovery from radiation damage[11]. This proposal has been derived from the fact that *Dr* accumulates significantly more manganese than other radiation sensitive microorganisms[19]. Additionally, it has been observed[20] that in a Wild-Type *Dr* growth, adding manganese before exposing a growth to Methyl viologen (see in 1.2), protected the cells against the oxidative stress caused by this compound. Despite this, the mechanism through which manganese confers this protection to the cells has not been fully understood.

## 1.2 Oxidative stress

Oxidative stress has been a challenge to define ever since it was started to be used as a term for when there is an excess of oxidants versus antioxidants in a living system, caused by the rate of production of ROS (or the other agents previously discussed) being much higher than their detoxification[21,22]. This might happen due to external stress or due to some defect in the cell's antioxidant machinery[23].

Oxidative stress induced by ROS causes deleterious effects in every organism. These ROS can be generated endogenously, by a cell's metabolism, through for example the aerobic respiration[24] which as a side effect may lead to the generation of different types of ROS like hydroxyl and superoxide radicals or even Hydrogen peroxide ($H_2O_2$)[25]. In equation 1.1 it is shown the complete reduction reaction of oxygen. If this reaction is not completed it will lead to the formation and accumulation of ROS.

These very reactive and unstable molecules can, if not controlled, cause damage to several types of macromolecules, e.g. DNA single or even double strand breaks, lipid peroxidation, destabilizing the cell's membrane, and damage to [Fe–S] clusters, which might lead to a loss of function of the protein[26,27].

Moreover, the oxidation of the Fe (II) into Fe (III) in the presence of $H_2O_2$, known as the Fenton reaction[28] (equation1.1), can also lead to the formation of the hydroxyl radical. ROS can be, as

well, generated by external stress agents, like Infrared and Ultraviolet radiation and desiccation, as will be discussed in 1.3.

$$O_2 \rightarrow O_2^- \rightarrow H_2O_2 \rightarrow OH^{\cdot} + H_2O \rightarrow 2\,H_2O \qquad \textit{equation 1.1}$$

$$Fe^{2+} + H_2O_2 \rightarrow Fe^{3+} + \cdot OH + OH^- \qquad \textit{equation 1.2}$$

To prevent these events from happening, organisms have developed antioxidant agents which scavenge the ROS and reduce the possibility of having these deleterious effects in the cell. Besides ROS, there are other molecules which can cause this cell damage namely, reactive nitrogen species (RNS), reactive sulfur species (RSS), reactive carbonyl species (RCS) and even reactive selenium species (RSeS)[29].

There are several forms of external stress that can cause the loss of cell viability related to the increase of oxidative stress. This work focuses on three oxidative stress agents: $H_2O_2$, Paraquat (or Methyl Viologen) and Ultraviolet C radiation. The effects of these agents will be discussed in 1.3.

## 1.3 Types of external oxidative stress causing agents used in this thesis

As explained earlier, $H_2O_2$ is one of the agents involved in the generation of hydroxyl via the Fenton reaction and can also affect protein conformation. This molecule, as shown in Figure1.2-A, is able to enter freely through the cell's membrane[21] and has a half-life of 1.5 hours in aerobic soil metabolism conditions[30]. Due to its toxicity, bacteria have developed mechanisms of scavenging and degrading this molecule. Among them is catalase which is a key enzyme which degrades $H_2O_2$ molecules, converting them to oxygen and water, as seen in Figure1.3-B.

A

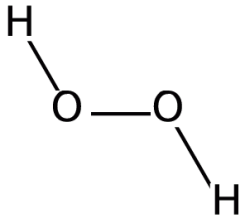

B

$$H_2O_2 + H_2O_2 \rightarrow O_2 + 2H_2O$$

Figure 1.2 - Structure of Hydrogen Peroxide (A) and catalase reaction (B).

Paraquat (1,1-dimethyl-4,4-bipyridinium dichloride), which structure is represented in Figure1.3, is an herbicide which consists of a bi-pyrimidine ring structure. Each of the rings has a quaternary amine and so paraquat has a charge of +2[31,32]. After entering the cell[33] this compound is reduced by any reductant in solution becoming a mono cation radical which then quickly reacts with oxygen forming superoxide anions. The superoxide anions have the half-life of 10 nanoseconds (ns)[34,35] and can oxidize NADPH, cytochrome c and even iron-sulfur proteins[32].

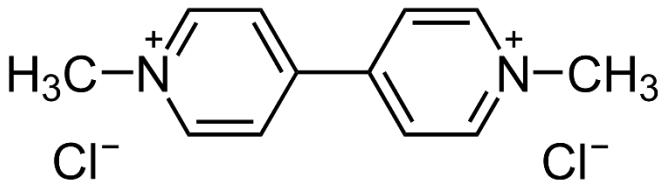

Figure 1.3 - Structure of Methyl viologen.

There are three types of Ultraviolet radiation: UV-A (315–400nm), UV-B (280–315nm) and UV-C (100–280nm)[36]. But not all the three types of ultraviolet radiation reach the surface of the Earth. The UV-C radiation is absorbed by the ozone layer due to its smaller wavelength and practically does not reach the Earth's surface. Therefore, the early studies of Ultraviolet radiation focused mainly on the UV-A and UV-B radiation, which reach the Earth's surface and have positive but also negative effects.

In more recent studies, the UV-C radiation has been shown to have a more bactericidal effects than UV-A and UV-B[37]. This is because of the different targets of the different ultraviolet radiation. The UV-C radiation damages DNA[38] creating pyrimidine dimers while the

ultraviolet radiation with a longer wavelength (UV-A and UV-B) targets lipids which will cause the destabilization of the cell's membrane, that can also lead to lethal effects[37]. Pyrimidines are the main target of the UV-C (mainly thymines) even though purines can also absorb the ultraviolet radiation but 10-fold less robustly[39].

Besides targeting DNA, UV-C radiation has been demonstrated to cause the formation of ROS[40]. The main UV induced oxidized damage is played by singlet oxygen; $H_2O_2$ and the superoxide anion ($O_2$- ). The hydroxyl radical may also be involved[41].

## 1.4 EndonucleaseIII: *Dr*EndoIII1, *Dr*EndoIII2, *Dr*EndoIII3

DNA is constantly being damaged, whether it is by endogenous or exogenous agents. Besides that, polymerases also commit errors, which need to be corrected in order to preserve the genetic information[42]. To ensure that DNA is preserved, bacteria have developed DNA repair systems. The five major DNA repair systems are base excision repair (BER), nucleotide excision repair (NER), mismatch repair (MMR), homologous recombination (HR), and nonhomologous end joining (NHEJ)[43]. Amongst them, the BER pathway is the most important cell protection system, repairing the oxidative DNA damage[44].

*Dr*'s genome possesses 11 genes that encode for DNA glycosylases and among them, three genes encode for EndoIII-like DNA glycosylases: *Dr*EndoIII1 (DR2438), *Dr*EndoIII2 (DR0289) and *Dr*EndoIII3 (DR0982)[45]. While most of the *Deinococcus* species encode for 3 EndoIII-like proteins most other bacteria only contain one gene encoding the EndoIII protein. The reason for *Dr* possessing three EndoIII proteins is not well understood, however they do not have redundant roles, as each of them have their specific characteristics and seem to serve different roles in stressed conditions[46]. Their amino acid sequence identity is also low (~30%).

These three enzymes, present in *Dr*, are involved in the DNA repair systems through the Base Excision Repair (BER) pathway. The BER pathway is a housekeeping system responsible for constantly repairing DNA damage, including oxidized nucleobases that if left unrepaired could compromise cell viability. BER is initiated with the recognition of damaged bases by DNA glycosylases, and removal from the DNA strand into the active site cavity, where the base is stabilized and then the N-glycosidic bond between base and sugar phosphate is cleaved. The DNA strand is then repaired with the help of the polymerase and ligase which

will introduce and ligate the right base to the strand, respectively[45]. This pathway is shown in Figure1.4.

EndoIII proteins are bifunctional glycosylases, showing AP-lyase activity (cleavage of the DNA backbone in the 3′ side of the abasic site), in addition to the N-glycosidic activity and both functions are coupled through a β-elimination reaction. The main substrate for EndoIII enzymes is thymine glycol (Tg)[45], which are non-mutagenic but blocks replicative polymerases. However, EndoIII also recognize and remove oxidized cytosine and uracil which are mutagenic and can cause C - T transition and C - G transversion[47].

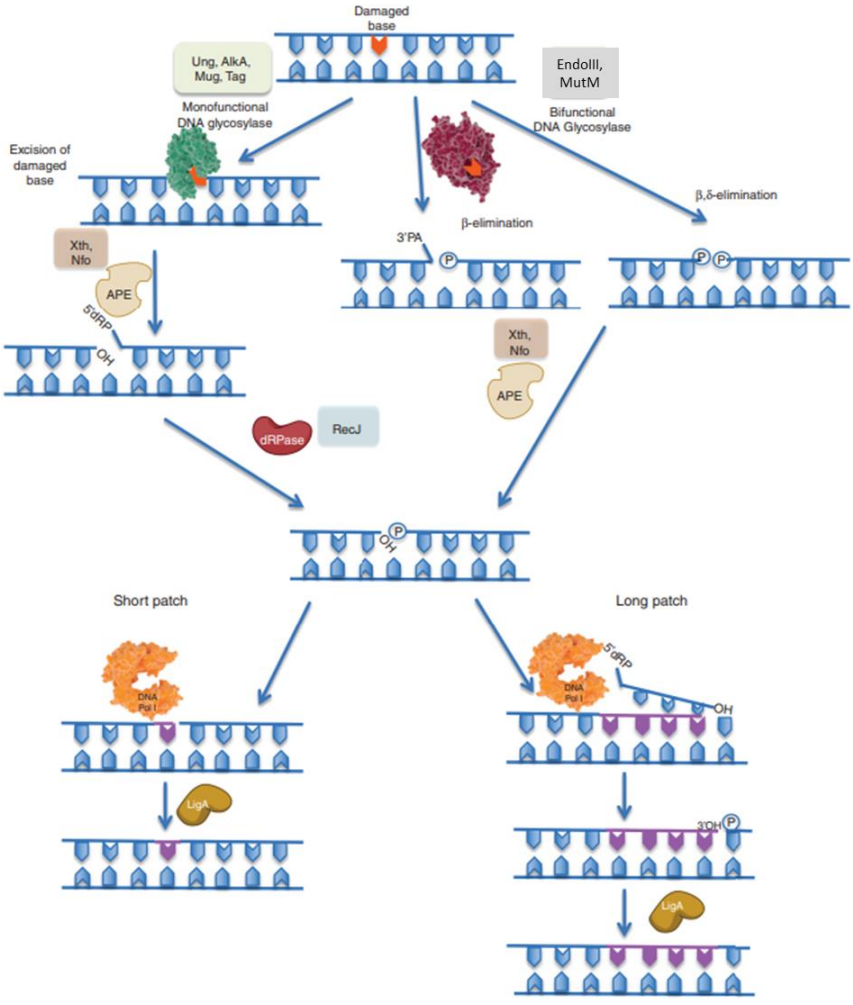


Figure 1.4– General scheme of the Base Excision Repair pathway in bacteria. Image adapted from [48].

So far, the crystal structure of EndoIII-1 and EndoIII-3 have been determined[46,49], and these structures are shown in Figure1.5. They consist of a two domain helical bundle structure, separated by a positively charged DNA binding cleft and belong to the Helix-hairpin-Helix (HhH) family of DNA glycosylases.

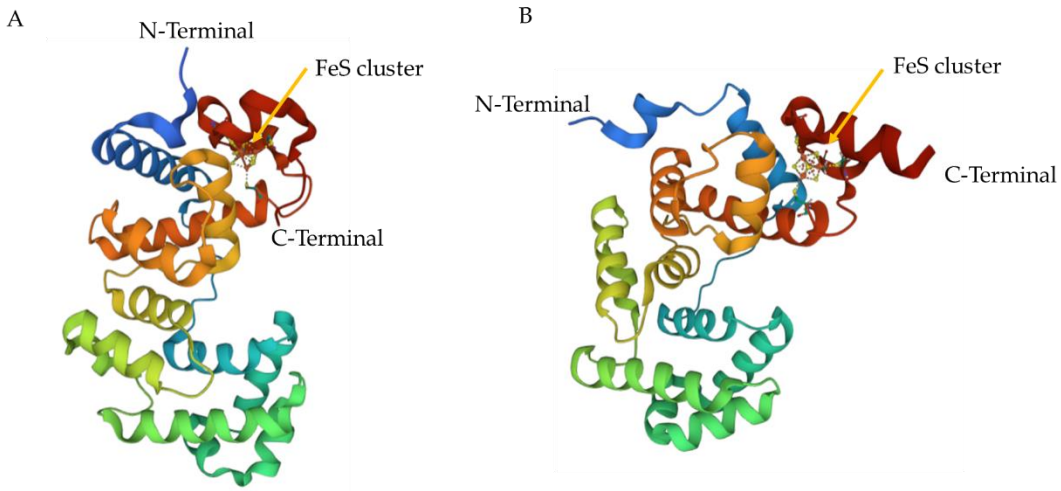


Figure 1.5 – Crystal structures of EndoIII-1 (A) and EndoIII-3 (B).
Images taken from PDB. EndoIII-1 (4UNF) and EndoIII-3 (4UOB).

These proteins possess an iron sulfur cluster [4Fe-4S], which role has not been completely understood. Early studies showed that the cluster was unreactive in solution and led to a suggestion that it might only serve a structural role. More recent studies have shown that the cluster can be redox activated when the protein binds to DNA or positively charged molecules[46].

It has been shown that EndoIII-1, in *Dr,* is more expressed under normal growth conditions, than EndoIII-2 and EndoIII-3 [25]. From activity assays, EndoIII-2 revealed the most AP-lyase and glycosylase activity, being proposed to act as a "workhorse" in the repair of the oxidized nucleobases[46]. EndoIII-1 even though being a bifunctional glycosylase, mainly demonstrated a monofunctional glycosylase activity, which might correspond to a secondary response to the repair of oxidized nucleobases and the repair to damage done to ssDNA. EndoIII-3 has a typical EndoIII fold but does not present any activity to the usual EndoIII DNA substrates. These two proteins (EndoIII-1 and EndoIII-3) have been proposed to exist in *Dr* to guarantee the repair of damaged bases, in cases of highly genotoxic stress, even though the role of EndoIII-3 is not completely understood[45].

## 1.5 Dps: Dps1 and Dps2

Besides the DNA repair system present in *Dr*, this organism also depends on a very efficient DNA damage protection system[50].

In *Dr* there are expressed two DNA protection during starvation (Dps) proteins: Dps1 (DR2263) and Dps2 (DRB0092)[51]. These proteins have a key role in binding to DNA, protecting it from the deleterious effects by ROS or by generating a supply of $Fe^{2+}$ for a quick detoxification of ROS[52]. This is due to their role on metal homeostasis, namely iron and manganese. The storage of iron, is key to prevent oxidative damage to macromolecules through the production of ROS via the Fenton reaction (see 1.2)[53].

Dps1 and Dps2 are present across *Deinococcus* species, namely in *D. gobiensis*[54]. There are other organisms that contain two genes for Dps-like proteins, such as, for example, *Bacillus anthracis* [55].

*Dr*Dps proteins belong to the ferritin family[56] as they share similar structures to these proteins. They are composed by 12 identical monomers, that form a hollow sphere with an internal cavity, as seen in Figure1.6. Both proteins possess a longer N-terminal than other Dps family members. This characteristic has been associated with the ability of them to form complexes with DNA[56].

These two proteins have been localized intracellularly, showing a different cell localization. This suggests that they play different roles in the DNA protection system. Dps2 has two dodecameric forms, one cytosolic and one associated with the membrane[20]. Dps1 might be involved in organizing the genetic material, as it has higher affinity to DNA than Dps2[17], while Dps2 might be involved in the protection against ROS[50] or in "Fe-trafficking"[20].

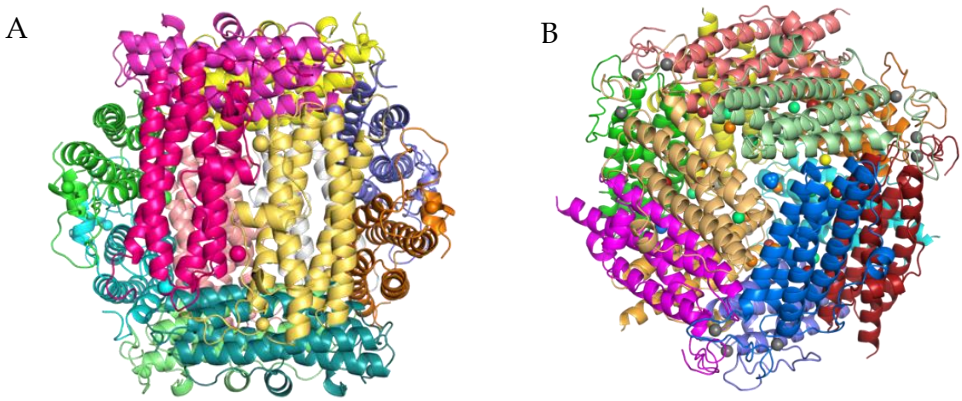


Figure 1.6 - Crystal structures of Dps proteins.
A) Dps1 – View through the 2-fold axis – 2C2F PDB B) Dps 2 - View through the 3-fold axis – 2C6R PDB.

## 1.6 PPK: PPK1 and PPK2

In order to withstand extreme doses of radiation, besides the DNA repair and protection systems, *Dr* possess a non-enzymatic system which play a key role as a protection mechanism after the exposure to radiation. This non-enzymatic system produces organic molecules which act as antioxidants and help in the response against ROS[57].

Inorganic polyphosphate (polyP) is a linear polymer, which is constituted by tens to hundreds of phosphate residues[58]. PolyP has been associated with several functions in bacteria, from storing energy, by acting as a kinase donor to form ATP and GTP[59], metal chelator, a regulator of stress and survival[60] and even acting as a chaperone to protect the structure of proteins[61]. Furthermore, polyP has been studied to chelate manganese ions, forming complexes, and this way, play a key part in the defense against oxidative stress, acting by protecting the proteome from suffering severe damage, playing a role as an antioxidant agent[61].

The proteins involved in the metabolism of inorganic polyphosphate, which is responsible for the synthesis of polyphosphate are the Polyphosphate kinase (PPK). *Dr* expresses 2 types of PPKs: PPK1 and PPK2, which do not share a significant sequence identity[62]. PPK1 generally synthesizes polyP from nucleoside triphosphates[62] while PPK2 preferentially consumes polyP to phosphorylate nucleoside mono or diphosphates[63], forming ATP. A general scheme of both reactions can be seen in Figure1.7. It has also been reported[60,64], that both enzymes can have the reverse activity in specific conditions, like the absence of one of the two enzymes.

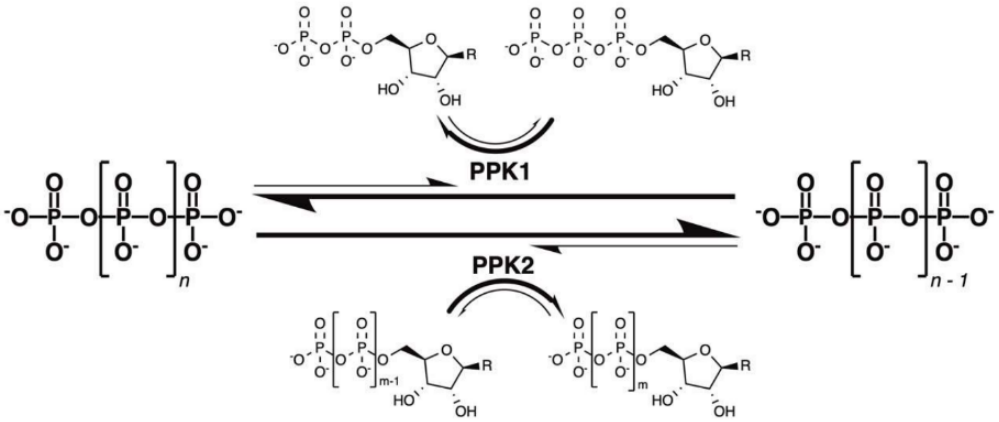


Figure 1.7 - Scheme of the reaction catalyzed by PPK1 and PPK2
Adapted from [62]

# 2

# OBJECTIVES

The first goal of this work was to establish a reliable protocol of constructing single, double, or even triple knockout mutants, of the EndoIII, Dps and PPK family of proteins, of *Deinococcus radiodurans*.

With those knockout mutants, oxidative stress and UV-C radiation assays were conducted to try and understand the roles of those family of proteins in the response against the extreme conditions used.

Lastly, a single amino acid mutated EndoIII-2 was expressed and purified. Crystallization was then performed with the goal of being able of determine the protein crystal structure.

# 3

# MATERIALS AND METHODS

## 3.1 Generation of knockout mutants – Tripartite ligation method by Phusion PCR and Homologous recombination

To construct *Dr's* knockout mutants, the technique used was replacing the target gene with an antibiotic resistance gene (Figure 3.1). To achieve this, the tripartite ligation method was used. It consists in amplifying three DNA fragments, an upstream and a downstream region of the target gene (~ 500 bp each) and an antibiotic resistance gene (selection marker) using Polymerase Chain Reaction (PCR) (see 2.1.1), ligate the three fragments and use it for transformation of competent *Dr's* cells. Upon transformation, the linear fragment will be integrated into the genomic DNA by homologous recombination which results in the replacement of the target gene with the selection marker. The tripartite ligation method can be done by using restriction enzymes and a ligase to connect these three fragments, but this proved to be very error friendly and sensitive. So, another method was used to obtain the three-pieced fragment, Fusion PCR[65].

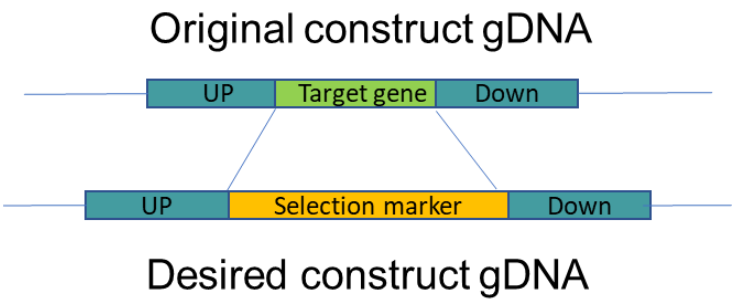


Figure 3.1 – Knockout mutant generation system by replacing the target gene with a selection marker, namely an antibiotic resistance gene.

The Fusion PCR method allowed the construction of this three-pieced-fragment without the use of restriction enzymes or a ligase. The primers designed to amplify the single fragments must have a tail homologous to the previous fragment allowing the amplified fragments to overlap each other and form a single three-pieced-fragment. Six primers are required to generate the fragment capable of knocking out a specific target gene (one pair for each fragment: forward and reverse). The primers used throughout this experimental work are shown in Table 3.1. To check if the designed primers had any GC clamp or hairpin formation, they were analyzed through PCR Primer Stats in the Sequence Manipulation Suite software[66]. The fusion was done with two fragments at a time, either joining the upstream fragment to the antibiotic resistance gene, or the antibiotic resistance gene to the downstream fragment. Only after two of the fragments were fused together, the merging of the third fragment was attempted. Initially in the fusion PCR, when joining fragment 1 and 2, no primers are added thus the fragments start to overlap due to the complementary regions and forms a template for the reaction. Thereafter, the two end primers (forward and reverse) of the target fragment are added to amplify that fragment. In the second step this procedure is repeated but now with fragment 1+2 and fragment 3. To confirm the results, the samples were analyzed by agarose gel electrophoresis (see in 3.1.2), to make sure they had the expected number of base pairs. Once this was assured, the fragments were purified from the gel (see in 3.1.3) and either used for the second fusion PCR step, or in the case of the final linear fragment, used for transformation of *Dr competent cells* (see in 3.1.4). The knockout mutants were selected by growing the transformants on solid media with antibiotics corresponding to the antibiotic resistance gene that replaced the target gene (see in 3.1.5). A scheme of this protocol is shown in Figure3.2. The confirmation of the knockout mutation was performed, as explained in 3.1.6.

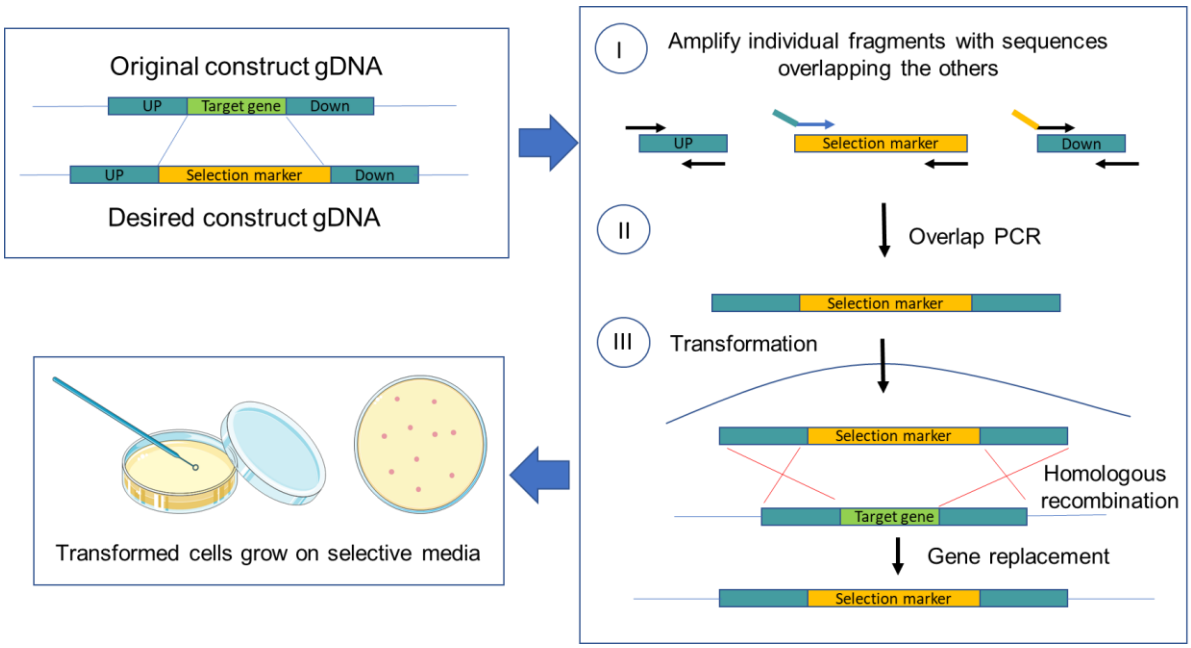


Figure 3.2 - Scheme of the generation of the knockout mutants

Table 3.1 - List of the primers used in the generation of knockout mutants. The underlined sequences were essential for the overlapping of the fragments, allowing the fragments to ligate through Fusion PCR

| | |
|---|---|
| EndoIII-2 Up FP | CGGCGGCGGGCAGTCCCAAG |
| EndoIII-2 Up RP | CTAGGCCAGAAGGCTTAGTG |
| EndoIII-2 Down FP | CTACGCCTGAATAAGTGCGGCCGCGTCGGTGGAGCATGTCGAGGG |
| EndoIII-2 Down RP | GTCATCAGGGCGCTTTGCAC |
| EndoIII- 2 CAM FP | GGCCAGTCACTAAGCCTTCTGGCCTAGTCCCTTTGGAACGGTGCT |
| EndoIII-2 CAM RP | GACGCGGCCGCACTTATTCA |
| EndoIII-3 FP | CCGTTGACCACGCCGATTTG |
| EndoIII-3 RP | ACTCGTTTCCGGACACGTTC |
| PPK1 Up FP | GGTCGCCAGCGCGGAAACTTT |
| PPK1 Up RP | TTAGCGCACGGCTGCCAAGCTG |
| PPK1 Down FP | CTCGAATTCACTGGCCGTCGAATGAGGGTTCGCTAGACCTG |
| PPK1 Down RP | AAAAGGCTGGTGGTGGGACGA |
| PPK1 Hygro FP | GGCAGCCGTGCGCTAAATCTCAAGGAGATCCGTGTTTCAGTTAGCC |
| PPK1 Hygro RP | CGACGGCCAGTGAATTCGAG |

### 3.1.1 PCR

This technique consists of an enzymatic reaction of DNA amplification, in which it is possible to make billions of DNA copies of a single fragment. To run a PCR there are three important steps in its program: *denaturation* of the DNA into single strands (at 98ºC for the Phusion Polymerase (Thermo Fisher)), *annealing* of the primers to that single strand template (depending on the melting temperature of the primers), and *elongation* which allows the formation of the new DNA strands from the primers (at 72ºC for the Phusion Polymerase). Several components are key elements in the PCR sample such as the polymerase, the dNTPs (Thermo Fisher), the designed primers, the DNA template and in some cases DMSO (Thermo Fisher), for high GC content DNA, because it useful in disrupting secondary structures of DNA[67]. An example of a PCR reaction used is shown in Figure3.3-A. This reaction was submitted to changes when a higher concentration of the template or no DMSO was needed.

In this work the polymerase used was the Phusion Polymerase, thus the conditions used for the PCR were the ones recommended for this polymerase by the polymerase manufacturer (Thermo Fisher). The polymerase kit comes with two different buffers (GC and HF) and some experiments were conducted to determine which gives the best amplification of the target PCR products. The most frequently PCR mix and program used in this work (standard PCR condition), is shown in Figure3.3-B. Due to the properties of the different primers, the annealing temperatures were varied, spanning from 50ºC and 65ºC. The time of the elongation step also varied according to the different fragment size that was being amplified, based on the recommendations in the product manual provided by the product supplier. The PCR was performed in the Biometra PCR Thermal cycler T gradient from alfa gene followed by product formation analysis (size of PCR fragment) by agarose gel electrophoresis (see in 3.1.2).

A

| **PCR mix:** | |
|---|---|
| dNTPs (50x) | 1 µl |
| High fidelity buffer 5x (GC) | 10 µl |
| DMSO | 1.5 µl |
| Forward primer (10 µM) | 1 µl |
| Reverse primer (10 µM) | 1 µl |
| DNA template | 2 µl |
| Polymerase (phusion) | 0.5 µl |
| MilliQ $H_2O$ | 33 µl |
| Total | 50 µl |

B **PCR program:**

| | | |
|---|---|---|
| 98°C | 5 min | |
| 98°C | 30 sec | |
| **60**°C | 1 min | Repeat 29X |
| 72°C | 2 min | |
| 72°C | 7 min | |
| 4°C | indefinitely | |

Figure 3.3 - General PCR mix used (A); General program for the PCR reactions (B).

## 3.1.2 Agarose gel electrophoresis

Agarose Gel Electrophoresis is a technique used for DNA analysis and allows separating DNA fragment based on the number of base pairs the fragment contains. This separation is possible due to the appliance of an electrical field to the gel, causing the DNA, that has a negative charge, to migrate to the cathode. This migration will cause the larger fragments to migrate slower through the gel and the smaller fragments migrate faster resulting in a clear separation.

Here, this method was used to detect the presence of formed PCR products and confirm that the DNA fragments had the expected number of base pairs. It was always used an 1% agarose gel for this purpose and the samples were ran from 45 minutes to 1 hour at 90 to 100V.

The buffer used in this electrophoresis is the TAE buffer 1x. The recipe for TAE 50x is 2M of Tris base, 1M of acetic acid and 50mM of EDTA disodium salt dihydrate ($Na_2EDTA$).

50mL of TAE buffer 1x was added to 0.5 grams of agarose (Sigma-Aldrich) and then dissolved by heating up the solution in the microwave. 2.5 µL of Xpert Green DNA strain (20000x, Grisp) was added and poured into the agarose gel casting tray with the well forming comb already mounted and left to solidify. The marker used in every run was the 1kb ladder.

A Gel Doc EZ Imager from BioRad was used to visualize and image the formed PCR products after the agarose gel electrophoresis.

### 3.1.3 Purification of PCR products by gel extraction

After obtaining the desired DNA fragments, they were cut out of the agarose gel and purified using the QIAquick Gel Extraction Kit (QIAGEN) according to the user manual[68]. In short, the gel fragments were weighed, followed by addition of 3 volumes of Buffer QG (e.g., to 100 mg gel, 300 µL buffer were added). This mix was incubated at 50°C for 10 minutes and vortexed every 2 to 3 minutes, to help dissolve the gel. After that, 1 gel volume of isopropanol was added to the sample and mixed. The sample was then pipetted into the QIAquick column followed by a 1 min centrifugation at 15,700 xg in a tabletop centrifuge. 750µL of the Buffer PE was added to the column and centrifuged again at 15,700 xg for 1 minute. To remove residual ethanol, the centrifugation was repeated. After that, the flow-through tube was discarded and the column was placed in a 1.5mL Eppendorf tube. To have a concentrated sample, 20µL elution buffer were added to the center of the column and left incubating at room temperature for 4 minutes followed by a 1 min centrifugation at 15,700 xg. The concentration of the resulting purified DNA was measured with the absorbance at 260nm, using NanoDrop spectrophotometer (Thermofisher).

### 3.1.4 Preparation of *Dr* competent cells and transformation

Throughout this experimental work two different protocols were used for preparation of the competent cells. For the EndoIII-2 knockout mutation the competent cells were prepared by resuspending cultured *Dr* cells at an $OD_{600}$ (Optical density of 600nm) of 0.5 to 0.6 in 1mL of a TGY2x-$CaCl_2$-Glycerol medium, which consisted of 4.275mL of TGY2x, 150µL of $CaCl_2$ 1M

and 570µL of Glycerol 87%. The cells were then aliquoted in volumes of 100µL in pre-cooled Eppendorf tubes and stored at -80ºC.

When the desired PCR fragment for the generation of the knockout mutant was obtained, one aliquot of competent cells was thawed on ice and 100µL of Medium B (500µL of TGY2x and 15µL of $CaCl_2$ 1M) was added. Around 100ng of DNA was also added. The sample was incubated at 0ºC for 25 minutes followed by an incubation for 30 to 60 minutes at 30ºC and shaking at 150 rpm (ABALAB). 1mL of TGY2x was then added to the sample and it was left incubating for 5 hours at 30ºC and 150rpm shaking. Previously prepared TGY2x plates with chloramphenicol (3.5µg/mL) were used to plate the transformation mix. The mix was then spread throughout the plate using sterilized spherical beads. The plate was left incubating at 30ºC (WTC Binder).

Another protocol was used for the generation of the remaining knockout mutants[69]. In this protocol, the competence was achieved by adding 30mM of $CaCl_2$ to *Dr* cultures at 0.3-0.4 $OD_{600}$ and left incubating for 1 hour at 30ºC at 150rpm for 1 hour. Once the desired fragment was obtained, a range from 500-800ng of DNA was added to 1mL of $CaCl_2$ treated bacterial culture followed by an incubation on ice for 45 minutes. This transformation mixture was afterwards incubated on an orbital shaker at 30ºC for 30minutes at 150rpm. After that, it was 10-fold diluted and left incubating overnight, around 19 hours at 30ºC at 150rpm.

### 3.1.5 Selection of knockout mutants

The transformation mixtures were spread onto plates of TGY2x with and without the target antibiotic. 100µL and 500µL (spun down and resuspended in 100µL of TGY) of the transformation mixture were plated. The mix was then spread throughout the plate using sterilized spherical beads. The transformation mixtures were incubated at 30ºC. After some days, some independent colonies that appeared in the plates were picked and grown in TGY and used for preparation of freeze stock cultures. Following this protocol, ΔEndoIII-2, ΔEndoIII-1/2, ΔEndoIII1/2/3, ΔEndoIII-2/Dps1, ΔPPK1 and ΔPPK1/2 were constructed.

### 3.1.6 Confirmation of knockout mutants

To confirm that the original gene in the *Dr* cells were replaced with the knockout construct, genomic DNA was purified from the obtained knockout mutants and used for amplification by PCR and the end primers of the UP and DOWN fragments and PCR fragment analysis by agarose gel electrophoresis. A comparison of the number of base pairs in the region of the target gene in the genome between the wild-type (WT) genome and the knockout mutant's genome was performed. As the gene encoding the antibiotic resistance in all cases are larger than the gene it replaced an obtained larger PCR fragment from the genomic DNA of the knockout mutant indicated that the original gene had been replaced in this strain. These results are shown in 3.1.1. The genomic DNA of every knockout mutant was purified using the GenElute Bacterial Genomic DNA kits (Sigma Aldrich) according to the protocol provided with the kit.

## 3.2 Ultraviolet (UV) and oxidative stress exposure assays

The constructed knockout mutants were exposed to different concentrations of oxidative stress agents, hydrogen peroxide and methyl viologen, to try and understand the role of those proteins in the response against these stress agents. These knockout mutants were also exposed to different doses of UV-C radiation. Two growth mediums were used throughout this experimental work: M53 and TGY which are both rich mediums. M53 consists of 1% (w/v) of Casein Yeast Peptone (Sigma-Aldrich), 0.5% (w/v) of Yeast Extract (VWR), 0.5% (w/v) of NaCl (Merck) and 0.5% of Glucose (Carl Roth) 20% (w/v). TGY is composed by 1% (m/v) of Tryptone (VWR) and 0.5% (m/v) of Yeast Extract (VWR) and 0.5% of Glucose (Carl Roth) 20% (w/v). To prepare solid mediums 1.5% of Agar (Carl Roth) was added to the medium. This allowed to understand the difference in response depending on the medium.

To make sure that the cells were in the same growth phase and in the closest conditions possible between experiments, every experiment was performed using the same protocol. Two overnight pre-inoculates were done and on the third day the experiment was performed. On this day, an inoculate was prepared with a starting $OD_{600}$ of 0.5 and left incubating at 30ºC, 150 rpm until it reached the $OD_{600}$ of 2.0. Once it reached that OD the assays were conducted.

### 3.2.1 Ultraviolet radiation exposure assays

8 different dilutions ($10^{-1}$ to $10^{-8}$) of culture of an $OD_{600}$ of 2.0, which corresponded to the early exponential phase of growth (see in FigureA 1 and 2), in two different mediums (TGY and M53), were plated in petri dishes in drops of 5µL and then exposed to UV-C radiation for a specific amount of time. Two replicates in the same plate were used as well as two plate replicates. The drops were placed in the center of the plate in two lines (see in Figure3.4-A). This entire experiment was performed in a laminar flow chamber in order to be able to have the plates open, so that the plastic lid wouldn't interfere with the sample exposure to UV-C radiation (see in Figure3.4-B). To guarantee and stabilize the intensity of the UV lamp (Analytikjena) an UVX radiometer (Analytikjena) was used, that was placed directly besides the plate, aligned with the drops. The plates were then exposed, from 0 to 60 seconds, to a 3 milliWatt per square centimeter ($mW/cm^2$) intensity. The irradiated cells were then left incubating at 30ºC for three days.

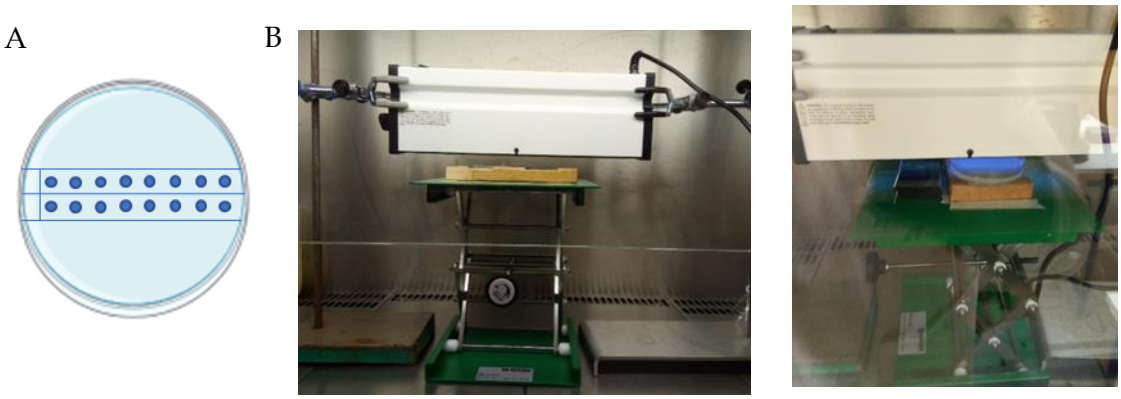


Figure 3.4 - Scheme of the UV-C assays. The plate with the drops with different dilutions (A) and the set up assembled in the laminar flow chamber (B).

In the results presented further ahead the units used are fluence units, Joules per square meter (J/m2). As previously stated, the dosimeter, that was at the same distance of the UV lamp as the drops, measured a $3mW/cm^2$ intensity. This result is then converted into $J/s.m^2$ corresponding to the fluence calculations for the UV-C assays (see in Equation 3.1). Once multiplied by the time of exposure (in seconds), the units are of $J/m^2$.

$$\frac{mW}{cm^2} = 10\frac{J}{s.m^2} \qquad \textit{equation 3.1}$$

### 3.2.2 Oxidative stress exposure assays

Once the inoculate reached $OD_{600}$ of 2.0, which corresponded to the early exponential phase of growth (see in FigureA 1 and 2), 100µL of cells was placed in a corner of a square plate (120x120mm) of TGY and M53 previously prepared, supplemented, if required, with the correct concentrations of antibiotics and spread first diagonally and then horizontally across the surface of the plate using a cotton swab (VWR). This same process was repeated to the other 3 corners of the plate to guarantee the homogeneity of the plate. This entire experiment was performed in a laminar flow chamber, to avoid any possible contamination. 6 cotton discs (Prat Dumas), with 6mm of diameter were then placed, using a sterile clamp, in the plate, roughly at the same distance of each other. This process is seen in Figure3.5. To each disc 20µL of different concentrations of the oxidative stress agent was added, except to the one disc that was used as a control, to which 20µL of sterilized MilliQ water was added. For each condition 3 replicates were done. The drops were then left to dry and the cultures were left incubating at 30ºC for three days. The results used for analysis were the diameter of the non-growing areas around the discs. These measures were done through the ImageJ program.

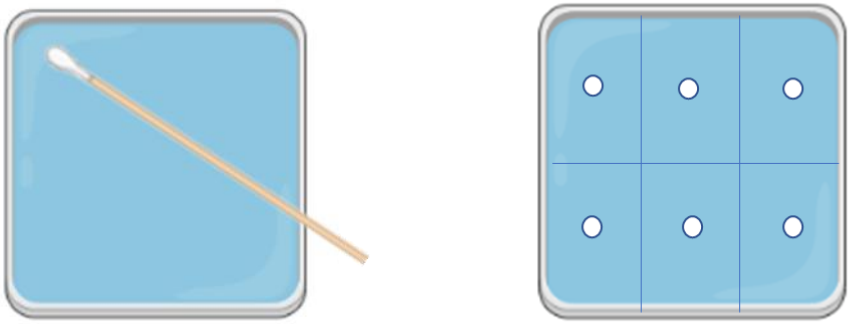

Figure 3.5 - Scheme of the plates of the oxidative stress assays.

## 3.3 Generation of EndoIII-2 mutant – site directed mutagenesis

Ala61 was substituted by Arg by altering the triplet code in the gene encoding EndoIII-2 by site directed mutagenesis. The mutation was introduced into the sequence of its gene that was

already inserted in a pDest14 vector (Gateway). In this plasmid the gene also contained a sequence encoding for a 6-histidine tag and a TEV cleavage site in the N-terminal of EndoIII-2. The aim of substituting Ala with Arg in this position in the protein sequence, was to obtain crystals of EndoIII-2 since the WT protein has not been crystallized yet. Regarding this experimental work, Luria Bertani (LB) medium was used, which consists of 1% (w/v) Tryptone, 1% NaCl (Merck) (w/v) and 0.5% (w/v) of Yeast Extract (VWR). To prepare solid mediums 1.5% of Agar (Carl Roth) was added to the medium.

Two overlapping primers: FpA61REIII2 5'GTGAGCGTGAACCGCGCCACTCCCGCCCTT3' and RpA61REIII2 5'AAGGGCGGGAGTGGCGCGGTTCACGCTCAC3' (mutation target region underlined) were designed in order to perform this mutagenesis using the NZYMutagenesis kit (NZYTech), and the protocol provided with the kit[70]. This kit generates a mutation in the target gene through PCR. After the PCR, 5µL of DpnI are added to the sample. DpnI is a restriction endonuclease that cleaves methylated sites. Since newly synthesized DNA does not have methylated sites, it is not digested. A volume of 10µL of the DpnI treated DNA was then added to 100µL of NZYstar competent cells, which are resistant to ampicillin. This mix was incubated for 30 minutes on ice. After that, the cells were heat shocked at 42ºC for 40 seconds. A volume of 900µL of Super Optimal broth with Catabolite repression (SOC) was added to the mix, which was then centrifuged at 2,300rcf for 1 minute. The supernatant (ca. 900µL) was discarded and the pellet was resuspended with the remainder volume. Into a plate of LB medium agar with ampicillin (100µg/mL) and chloramphenicol (35µg/mL), 100µL was pipetted and spread with the use of sterilized spherical beads. The plate was incubated overnight at 37ºC.

Colonies observed on the plate were then grown in 10mL of LB. Plasmid DNA (pDNA) was purified from those growths using the QIA Spin Miniprep Kit (QIAGEN). The obtained mutation was confirmed by sequencing (Eurofins).

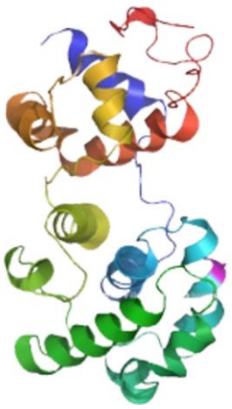

Figure 3.6 - Model of the EndoIII-2 protein.
The target site of the mutation is highlighted in pink.

## 3.4 Expression, purification and crystallization of EndoIII-2 mutant A61R

### 3.4.1 Expression of EndoIII-2 mutant A61R

The plasmid containing the gene encoding for the mutant was used to transform *E. coli* expression strain BL21(DE3)pLysS.

The transformation was done by adding 1µL of the plasmid (100ng/µL) to 100uL of BL21(DE3)pLysS cells and incubating the mixture on ice for 30 minutes. Then, the cells were heat shocked at 42ºC for 45 seconds and then immediately transferred to ice for 2 minutes. After that, 800µL of LB medium was added to the mixture and the mixture was incubated for 1 hour at 37ºC at 300rpm. Finally, 100µL and 200µL of the transformation mixture were spread in previously prepared LB+agar plates with ampicillin (100µg/mL) and chloramphenicol (35 µg/mL). The plates were left at 37ºC overnight and then stored at 4ºC. Additionally, 100µL of the remaining sample was used to start an overnight pre-inoculum of 20mL in LB medium with ampicillin (100µg/mL) and chloramphenicol (35 µg/mL).

In the next day, using the pre-inoculum, two 1-liter LB growths (10mL of the pre-inoculum added to each), with ampicillin (100µg/mL) and chloramphenicol (35 µg/mL), were incubated at 37ºC until it reached the $OD_{600}$ of around 0.6. Once this was achieved, 0.5mM of IPTG was added to the growth and then it was left incubating overnight at 20ºC. In the next morning,

the cells of both growths were individually harvested in 1L centrifuge bottles at 8.671 xg in Avanti J-26 XPI with JA-10 rotor for 20 min and then each collected pellet was stored at -20ºC.

### 3.4.2 Purification of EndoIII-2 mutant A61R

To proceed to the purification of the EndoIII-2 mutant, one of the pellets was thawed and resuspended in 20mL extraction buffer. The extraction buffer used is composed of 20mL of Buffer A (20 mM Tris-HCl, 250 mM NaCl, 10 mM Imidazole), 1 tablet of EDTA-free protease inhibitor (Merck), 1mM of $MgCl_2$, 1µg/mL DNase (Merck) and 0.1mg/mL of Lysozyme (Sigma-Aldrich). Then, to lysate the cells, 3 cycles of freeze (liquid nitrogen) and thaw (water bath at 22ºC) were performed.

After the freeze/thaw cycles, the sample was centrifuged at 39.191 xg in Avanti J-26 XPI with the JA25.50 rotor for 30 minutes at 4ºC. The resulting supernatant (~20 ml) was collected and filtered with using a 0.1 µM size low protein binding filter (VWR) and used for purification.

#### 3.4.2.1 Affinity chromatography

The purification protocol consisted of two affinity chromatography steps: His-Trap HP column (1 ml, Cytiva) followed by Heparin HP column (5 ml, Cytiva). The protein was purified using an AKTA explorer (Cytiva). Every buffer that is used during the purification has to be filtrated and degassed and the pumps and valves must be washed with water and 20% ethanol before and after each run. In order to avoid contaminations of the purification system, the machine and all columns are left in 20% (v/v) ethanol after use.

The His-Trap column binds to Histidine tags and all the proteins that do not have a His-tag goes through the column upon applying the sample to the column. To release the proteins with Histidine tags from the column, a buffer containing imidazole (which has a higher affinity to the column material than the proteins) is added to the column. Two buffers are used: Buffer A (50 mM Tris-HCl pH 7.5, 150mM NaCl +10mM Imidazole) and Buffer B (Buffer A + 0.5 M Imidazole). Buffer A is called binding buffer and it is used as equilibration buffer and washing buffer, as this buffer is added to the column prior to the purification (called equilibration), to prepare the addition of the protein solution, and is used to wash out the proteins without

Histidine tags before releasing the Histidine tagged proteins (purified protein) from the column material. Buffer B is called elution buffer because it is the buffer that is used to elute the Histidine tagged protein from the column material by adding an increasing amount of imidazole to the column material. Proteins which are weakly bound to the column, are eluted first (*E.coli* proteins with Histidine tag like properties), while the proteins with strong binding to the column material are eluted with high concentration of imidazole (usually recombinant proteins with Histidine tags).

The Heparin column is used to separate protein solutions based on its overall ionic charge, and is usually used to remove DNA from DNA binding proteins, as the column matrix is positively charged[71,72]. The elution of proteins was made according to the increasing ionic concentration. Thus, the two buffers used are: Binding Buffer-Buffer C (50mM Tris-HCl pH 7.5, 150mM NaCl) and Elution Buffer - Buffer D (50mM Tris-HCl pH 7.5, 1M NaCl). In this case a gradient of increasing NaCl is used to elute the proteins from the column matrix (increasing ionic strength) by increasing percentage of Buffer B injected through the column.

A HisTrap HP column (1 mL) connected to the AKTA explorer system was used in the first purification step. The Flow rate was 1 ml/min and 20mL of sample was loaded onto the column and a linear gradient from 5% of Buffer B to 100% of B for 20 Column volumes (CV) was used to elute the protein.

After that, fractions containing colored protein (EndoIII-2 possesses an iron-sulfur cluster which gives a brownish/orange color to the protein) was pooled and desalted by application to a 10 ml PD10 column equilibrated with buffer C. The resulting sample was thereafter loaded onto a heparin column (5 mL) and 1.5 mL fractions of this protein were collected automatically.

The different fractions that corresponded to the peak of Absorbance of 280 (with colored protein) were analyzed on an SDS-Polyacrylamide Gel Electrophoresis (SDS-PAGE) (see in 3.4.3) to confirm the purity and presence of the mutated EndoIII-2 protein in the samples. The fractions with pure protein were then pooled and concentrated with a centrifuge concentrator (Amicon, 10kDa), by centrifuging cycles at 2,880 xg in centrifuge 5804R (eppendorf), to around 20mg/mL in order to proceed to crystallization screens. The concentration was calculated using the theoretical extinction coefficient and measured in NanoDrop spectrophotometer (Thermofisher).

Figure 3.7 - AKTA explorer used in the purification steps of EndoIII-2 mutant.

### 3.4.3 SDS Polyacrylamide Gel Electrophoresis (SDS-PAGE)

This technique is used for protein analysis and separate proteins based on their molecular mass, using polymerized acrylamide which forms a mesh like matrix. In SDS-PAGE, the proteins are denatured. Denaturing conditions, such as adding β-mercaptoethanol and heating the samples, are used in order to break noncovalent bonds of native proteins and give them all a negative charge, which is caused by Sodium Dodecyl Sulfate (SDS). Macromolecules with a higher molecular weight migrate slower than low molecular weight proteins during the run of the gel.

The runs were about 1 hour long at 180V, without allowing the bromophenol blue, which is the dye present in the sample buffer, to reach the bottom of the gel.

The recipes used for the 12.5% gels are shown in Table3.2 and Table3.3. The running buffer used is composed by 0.25M of Tris-base,1.92M of glycine, 35mM of SDS, dissolved in bidistilled $H_2O$ ($ddH_2O$). The SDS-PAGE Loading buffer 4x used is composed by 0.2M of Tris-HCl pH6.8; 0.277M of SDS; 8% (w/v) of Glycerol; 5.7M of β-mercaptoethanol and 0.1% (w/v) of bromophenol blue. The samples were boiled at 95ºC for 5 minutes before loading them into the gel in order to fully denature the sample.

After each run, to be able to visualize the protein bands in the gel, Blue Safe (NZYtech) was added directly to the gel and left incubating at room temperature until the bands were clearly visible. Once this happened, the Instant Blue was replaced by $ddH_2O$.

Table 3.2 - Recipe of 12.5% resolving SDS-PAGE.

| Resolving Gel 12.5% | | | | | |
|---|---|---|---|---|---|
| $H_2O$ (mL) | Acrylamide Mix (mL) | 1.5M Tris-HCl pH8.8 (mL) | SDS 10% (µL) | APS 10% (µL) | TEMED(µL) |
| 2 | 1.25 | 1.7 | 50 | 50 | 2.5 |

Table 3.3 - Recipe of 4% stacking SDS-PAGE.

| Stacking Gel 4% | | | | | |
|---|---|---|---|---|---|
| $H_2O$ (mL) | Acrylamide Mix (mL) | 1.5M Tris-HCl pH6.8 (mL) | SDS 10% (µL) | APS 10% (µL) | TEMED(µL) |
| 0.335 | 0.625 | 1.5375 | 25 | 25 | 2.5 |

### 3.4.4 Crystallization of EndoIII-2 mutant A61R

Protein Crystallization is a method used to obtain the three-dimensional structure of proteins. To make it possible to happen, the protein solution is mixed with a high variety of precipitants and it can lead to nucleation of crystals (ordered repetition of identical units). Therefore, initially it is setup several experiments using a nano-crystallization robot and testing different commercially sparse matrix screens (96 well plate with different reagents in each well). In addition, different ratios of the protein solution and the crystallization condition can also be tested, in order to try different conditions in which crystals may appear. The drops are then monitored using a Stereo microscope (Leica), and in case protein crystals are obtained, the condition is manually optimized using 24-well plate. The crystals are then tested using an X-ray source, and the X-ray diffraction of these organized structures creates a diffraction pattern which can, through several mathematical analysis, as the Fourier Transformation, decipher a protein structure. Although we have to bear in mind, in order to obtain the 3D protein structure, it is important to have information on the phases, which is known as the "phase problem". In the current work, the plan is to use the Molecular Replacement method to obtain information on the phases, using the model structures of other EndoIII, namely EndoIII-1 (4UNF) and EndoIII-3 (4UOB) proteins from *Dr.*

X-ray crystallography is dependent on acquiring crystals of the macromolecule, and not simply crystals, but crystals of enough size and quality to permit accurate data collection. The quality of the final structural image can be directly determined by the perfection, size, and physical properties of the crystal.

Three types of crystallization screens were used in this work: Morpheus (Molecular Dimensions), Index (Hampton Research) and JCSG+ (Molecular Dimensions) and three different ratios of protein:crystallization solution were used 1:1, 1:2 and 2:1. The entire process of mixing the protein with the reagent and making the different drops in the plated was automated by the Mosquito LCP (ttplabtech). The experiments where then left in a room with a controlled temperature of 20$^{o}$C. The observation of potential crystal formation is done using a Stereo microscope (Leica).

# 4

# RESULTS

## 4.1 Generation of knockout mutants – Tripartite ligation method by Fusion PCR and Homologous recombination

### 4.1.1 Generation of EndoIII-2 single, Dps1/EndoIII-2 and EndoIII-1/EndoIII-2 double knockout mutants

The target gene for the first knockout mutant was the gene encoding EndoIII-2. To generate knockout mutants, as explained before (see 3.1), the first step is the amplification of three individual fragments needed for the Fusion PCR: the upstream (UP) and the downstream (DOWN) region of the target gene and the antibiotic resistance gene (CAM). In this case, the fragments should consist of 466bp, 529bp and 1200bp, respectively, and result in a full-length fragment (once the three fragments are ligated) consisting of about 2.2kbp.

Our results showed that the three individual fragments were successfully amplified using the PCR conditions described in 3.1.1 (Figure 4.1). In the lane of the chloramphenicol resistance gene, two additional unspecific PCR products are observed. They may have occurred due to similar annealing sites for the primers in the genomic DNA and could probably have been eliminated by increasing the annealing temperature to allow for only specific primer binding to the DNA. The three fragments were purified from the gel and had a concentration of around 20ng/µl. In the same gel, two gDNA samples were analyzed in order to check their purity.

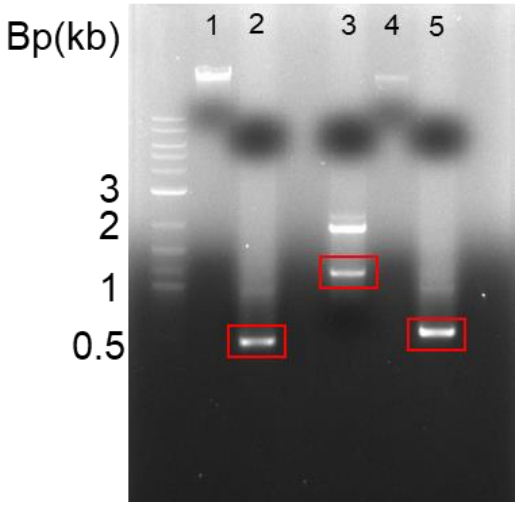


Figure 4.1 – 1% Agarose gel of different individual fragments obtained though PCR.
Amplification of the three single fragments (boxed in red) required for the generation of the knockout mutant: the upstream fragment (Up), the chloramphenicol resistance gene (CAM) and the downstream fragment (Down). Lane 1 and 4: WT gDNA; Lane 2: Up; Lane 3: CAM; Lane 5: Down.

In order generate one linear fragment for integration into the genomic DNA, the three purified fragments were ligated using two Fusion PCR reactions. These two PCR conditions were done using the standard PCR protocol, described in 3.1.1, with the only difference that the first PCR reaction did not have any primers, to allow the overlapping of the two fragments to occur, generating a template for the final PCR reaction. As seen in Figure 4.2-A, the target fragment of around 1600bp was only obtained in the Fusion PCR reaction where the upstream fragment was ligated to the chloramphenicol resistance gene. That fragment was cut out of the gel a purified to 7ng/µL and used in a second Fusion PCR reaction using the same condition as before. This time the Upstream-Chloramphenicol fragment was ligated to the Downstream fragment and resulted in the generation of a 2.2 kb fragment as expected (Figure 4.2-B). The fragment was cut out of the gel and purified to around 4ng/µL. To obtain more quantity of the complete fragment, a third PCR reaction, using the standard condition and the purified ligated linear fragment as a template and the end primers from the up and down fragment was conducted (Figure 4.2-C).

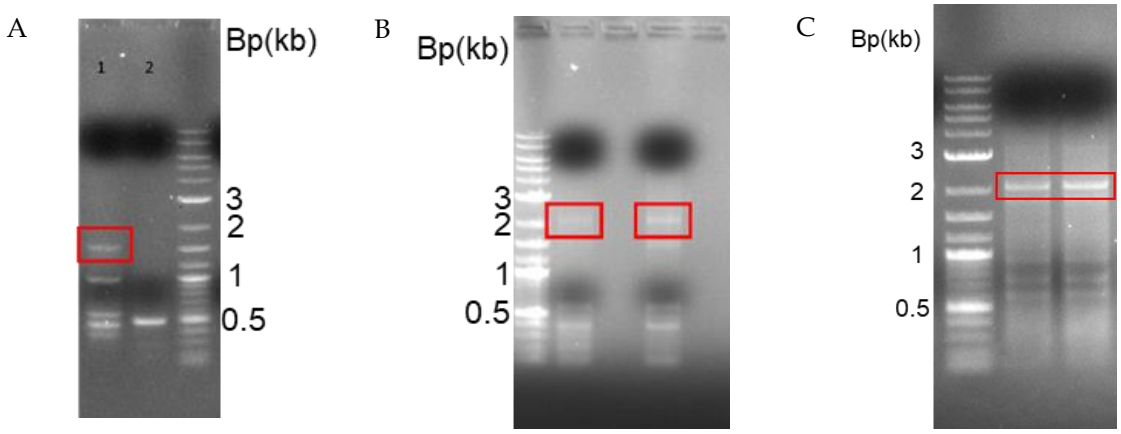


Figure 4.2 – 1% agarose gels with PCR products obtained by Fusion PCR.
A) Generated PCR products after Fusion PCR reaction of the upstream fragment (UP) (lane 1) to the chloramphenicol resistance fragment (CAM) and and the Downstream fragment (Down) to the chloramphenicol resistance fragment (CAM) (Lane 2), B) Generated PCR product of fusion of the Down fragment to the Up-CAM fragment and C) Generated Fusion PCR product of the UP-CAM-DOWN linear fragment. Fragments with expected sizes are boxed in red. Results of PCR presented by agarose gel eletrophoresis.

This fragment was then used to transform competent cells of *Dr* to generate the EndoIII-2 single knock out mutant. The same fragment was used to transform as well, competent cells of two *Dr* knockout mutants (ΔDps1 and ΔEndoIII-1) which already existed in the lab, in order to generate double knockout mutants (ΔEndoIII-2/Dps1 and ΔEndoIII-1/-2).

To select the cells with the EndoIII-2 knockout mutation, the culture was plated in TGY solid medium with Chloramphenicol (3.5µg/mL). These plates were then stored at 30ºC, and colonies appeared 5 days after the plating, as shown in Figure4.3. The method firstly used to generate ΔEndoIII-2, showed to take several days for any colonies to appear. For this reason, the protocol was altered to include a longer incubation time (overnight growth) of the transformation mix prior to plating on the selective medium (TGY2x with the respective antibiotics) and by adding more of the DNA fragment to the competent cells for the generation of the double knock out mutants. This change resulted in a clear difference in transformation efficiency between the EndoIII-2 mutant and the EndoIII-1/2 and Dps1/EndoIII-2 knockout mutants. In the case of the double mutants, as ΔDps1 and ΔEndoIII-1 were resistant to kanamycin, this antibiotic was also added to the plates (6µg/mL). As a control, and to confirm that the WT bacteria was indeed sensitive to the antibiotics, at the concentration used, 100µL of WT growths was plated in TGY with chloramphenicol, hygromycin and kanamycin. Since

no colony grew in the plates, as seen in the FigureA 3, with the antibiotics, it confirms that the WT is sensitive and so the colonies obtained in the selective plates correspond to the knockout mutants.

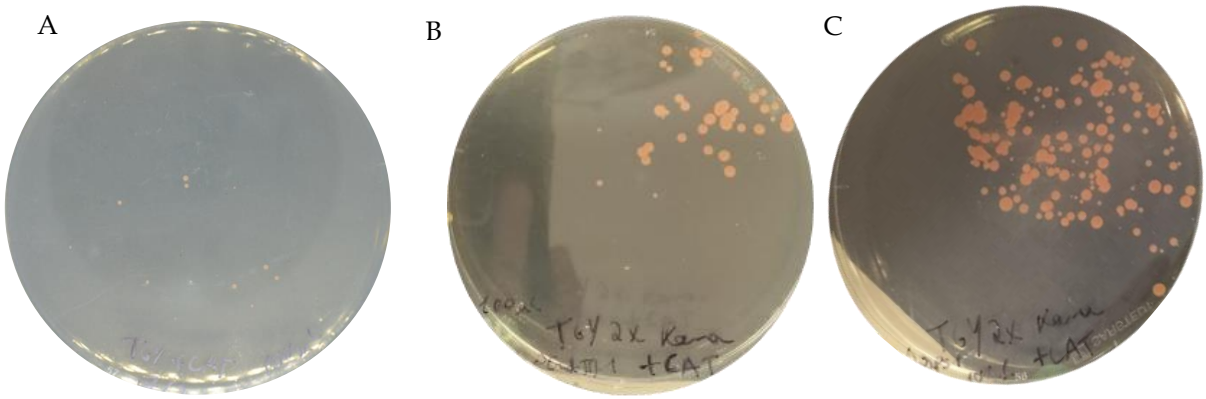


Figure 4.3 - TGY2X plates with the transformants, and the respective antibiotics.
A - ΔEndoIII-2 (chloramphenicol), B - ΔEndoIII-1/-2 (chloramphenicol and kanamycin) C - ΔEndoIII-2/Dps1 (chloramphenicol and kanamycin).

To confirm that the colonies that were growing in the selective media were *Dr*, one colony was picked from each plate and observed in the microscope (Figure4.4). The results demonstrated that the cells indeed presented the usual morphology of *Dr*.

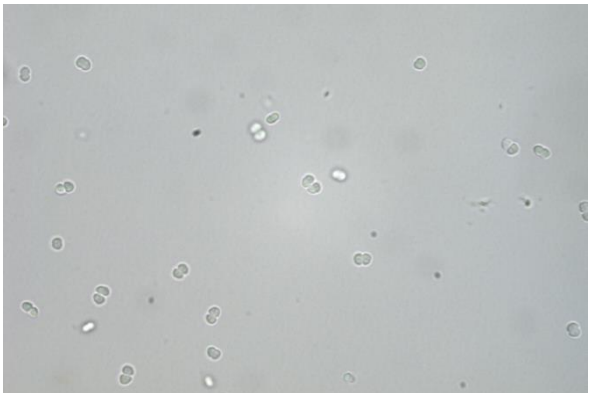

Figure 4.4 – Optical microscopy images of the EndoIII-2 knockout mutant, isolated from an individual colony from figure 4.3-A.

In order to confirm that the target gene had been replaced with an antibiotic resistance gene, the size of the EndoIII-2 region in the genome of the generated knockout mutant was compared with the same region in the genome of *Dr* WT by PCR. The PCR conditions used were the standard ones, shown in 3.1.1 and the primers used were the end primers: EndoIII-2

Up FP and EndoIII-2 Down RP, also presented in 3.1.1. The results (Figure4.5) showed that, as expected, the EndoIII-2 region was bigger in the genome of the knockout mutant (2.2 kb) than for the WT's *Dr* genome (around 1.7 kb). This is because of the replacement of the EndoIII-2 gene, which has 678bp, by the chloramphenicol resistance fragment which has 1200bp.

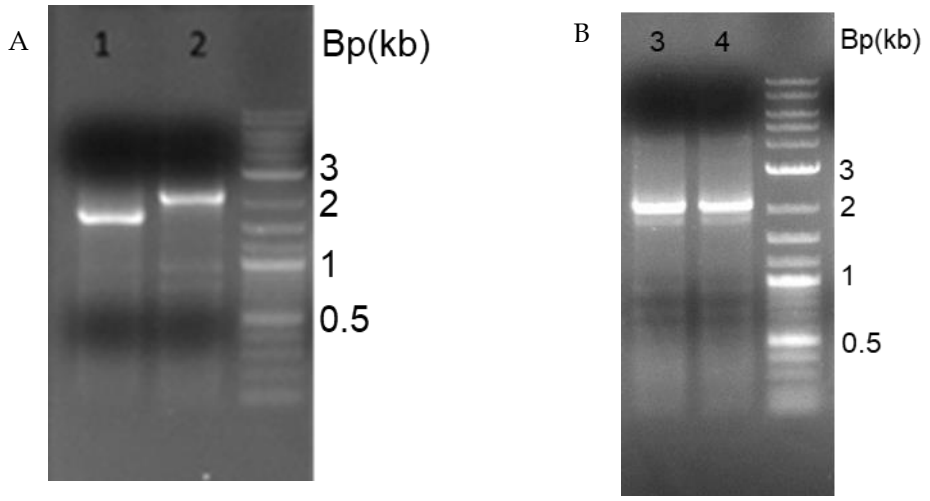


Figure 4.5- 1% Agarose gel used to compare the PCR results from confirmation of chloramphenicol gene insertion. A) The number of base pairs in the region of the EndoIII-2 gene was compared, using WT gDNA, lane 1, which corresponds to the original construct (around 1.7 kb); In lane 2 is the same region with the EndoIII-2 knockout mutant gDNA (around 2.2 kb) as a DNA template, which corresponds to the desired construct; B) In lane 3 and 4 it is shown the same region in the genome of the EndoIII-2/Dps1 and EndoIII-1/EndoIII-2 knockout mutants.

### 4.1.2 Generation of the EndoIII-1/-2/-3 triple knock out mutant

To construct the triple mutant, a linear fragment of the EndoIII3 region (including up and down regions) of a ΔEndoIII3 knock out mutant, that was also available in the lab, was amplified and used for transformation of the double mutant. Thus, only two primers were designed, to amplify the target fragment, which was already present in the genome of the EndoIII-3 knockout mutant.

Initially, no PCR product was observed in the agarose gel analysis, thus the annealing temperature was changed and increased gradually from 50ºC to 65ºC. However, still no product was observed. As this was not solving the problem, we hypothesized that, DMSO, which was part of the standard PCR mix, could be a plausible cause for the lack of PCR product. Thus, two parallel PCR mixes were prepared with the only difference being the presence of DMSO, in one, and the absence of DMSO in the other. From the results shown in Figure4.6, it is clearly visible that the PCR reaction without DMSO resulted in the generation of a PCR product, while the sample with DMSO did not. This compound was, probably,

causing deleterious effects in the PCR, possible due an interference of DMSO in the reaction or because the reagent was old and possibly degraded.

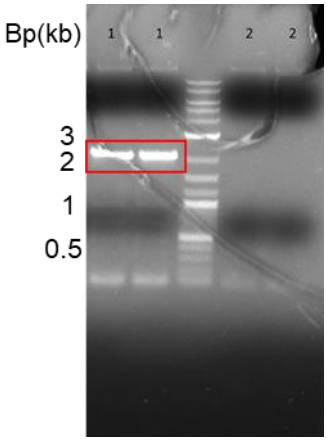


Figure 4.6- 1% Agarose gel used to show the results from PCR.
The target fragment for the EndoIII-3 knockout mutation, was amplified without DMSO (lanes 1) and with DMSO (lanes 2).

Once the fragment was purified, it was used to transform the double knockout mutant of EndoIII-1 and EndoIII-2, which was already resistant to Chloramphenicol (3.5µg/mL) and Kanamycin (6µg/mL), following the protocol explained in 3.1.4. The transformation mix was then plated in two different TGY2X plates with Hygromycin (50µg/mL). In one, Figure4.7-A, 100µL were added to the plate while in Figure4.7-B, the pellet of 500µL of the transformation mix was resuspended into 100µL and spread in the plate.

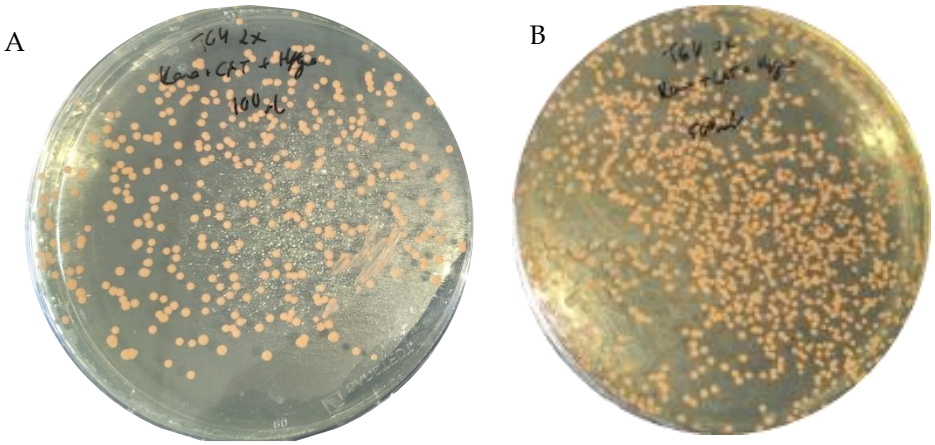


Figure 4.7 - TGY2X plates and the respective antibiotics with the knockout mutants of EndoIII-1/2/3. A - ΔEndoIII-1/2/3, 100µL of the transformation mix B - ΔEndoIII-1/2/3, pellet of 500µL of the transformation mix resuspended in 100µL.

In order to confirm that the EndoIII-3 gene had been replaced with the Hygromycin resistance gene, the size of the EndoIII-3 region in the genome of the generated knockout mutant was compared with the same region in the genome of *Dr* WT by PCR. The PCR conditions used were the standard ones, shown in 3.1.1 and the primers used were the end primers: EndoIII-3 Up FP and EndoIII-3 Down RP, also presented in 3.1.1. The results (Figure4.8) showed that, as expected, the EndoIII-2 region was bigger in the genome of the knockout mutant (around 2.2 kb) than for the WT's *Dr* genome (around 1.7 kb). This is because of the replacement of the EndoIII-3 gene, which has 783bp, by the Hygromycin resistance gene which has around 1200bp. The sizes of the Up and Down were, respectively, 473bp and 451bp.

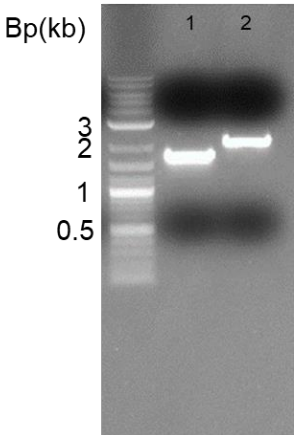


Figure 4.8 Confirmation of the replacement of the EndoIII-3 gene with the Hygromycin resistance gene. The number of base pairs in the region of the EndoIII-3 gene was compared, using WT gDNA, lane 1, which corresponds to the original construct (around 1.7 kb); In lane 2 is the same region with the EndoIII-1/2/3 knockout mutant gDNA (around 2.1 kb) as a DNA template, which corresponds to the desired construct.

### 4.1.3 PPK1 knockout mutation

In order to generate a PPK1 and a PPK1/2 double knockout mutants, 6 different primers were designed as previously explained in 3.1. Each pair of primers was used to amplify one individual fragment: either the Upstream region of the PPK1 gene (566bp), the Downstream region of the PPK1 gene (673bp) or the hygromycin resistance gene (1200bp).

Each individual fragment was amplified, by PCR using the standard PCR conditions, but initially only the Downstream and the Hygromycin resistance fragments were amplified, shown in Figure4.9-A. The two fragments amplified were then ligated by Fusion PCR (Figure4.9-B).

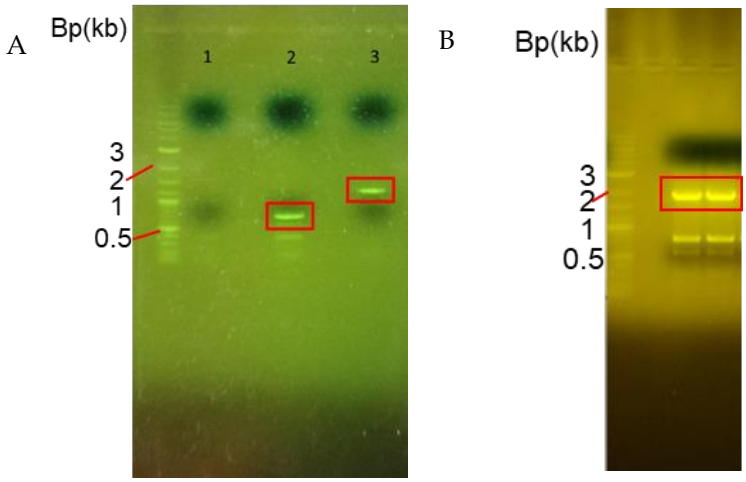


Figure 4.9 - 1% agarose gel with PCR products of the PPK1 knockout mutation fragment.
A – Amplification of the single fragments: upstream fragment (Up) in lane 1, downstream fragment (Down) in lane 2 and Hygromycin resistance gene (Hygro) in lane 3. B – Amplification of the Hygro-Down fragment, after ligation through Fusion PCR.

Due to the lack of the Upstream product in the first PCR, four different PCR mix were prepared, changing between the two different buffers for the Phusion Polymerase (HF and GC) and with and without DMSO (Figure4.10). The DMSO used in this experiment was from a fresh stock. These results show that DMSO was essential for the amplification of the Upstream fragment, and that both buffers seem to provide the same PCR yield.

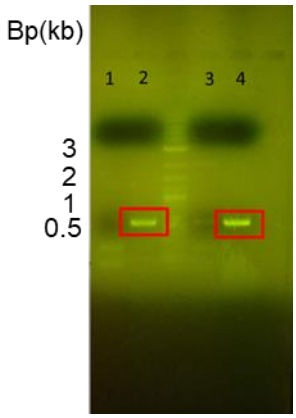


Figure 4.10 – 1% agarose gel with the attempts of amplifying the upstream fragment of the PPK1 gene. In lanes 1 and 2, the PCR mix was done using the buffer HF, while in lanes 3 and 4 the PCR mix was done using buffer GC. In lanes 2 and 4, DMSO was added to the PCR mixes.

The Upstream fragment was then purified and ligated through Fusion PCR to the Hygromycin-Downstream fragment (Figure4.11-A). In Figure4.10-B, it is shown the excision of the target fragment from the agarose gel.

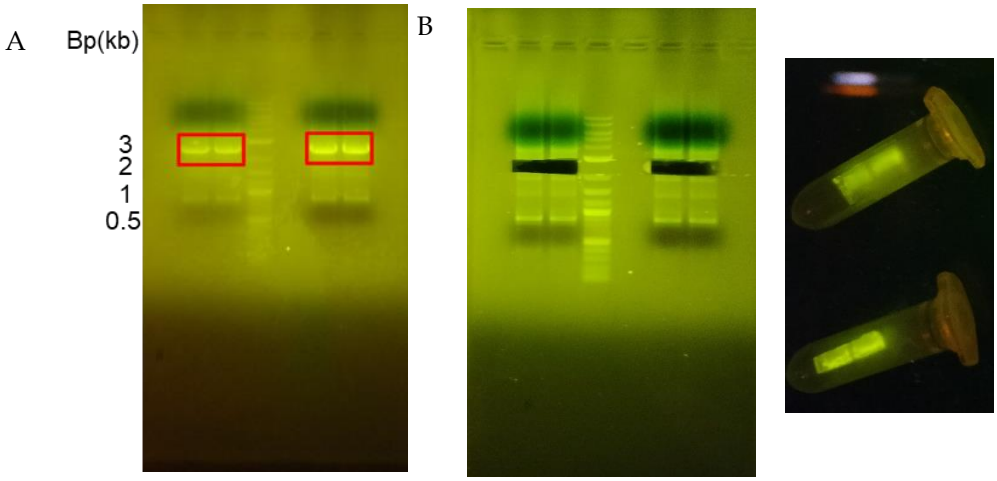


Figure 4.11 - Amplification and extraction of the target fragment used for the knockout mutation of the PPK1 gene.

Once the entire fragment was constructed, it was used to transform the WT and PPK2 knockout mutant which was already available in the lab, and which are resistant to Kanamycin (6µg/mL). The transformants were grown on TGY plates, with the respective antibiotics, as seen in Figure 4.12.

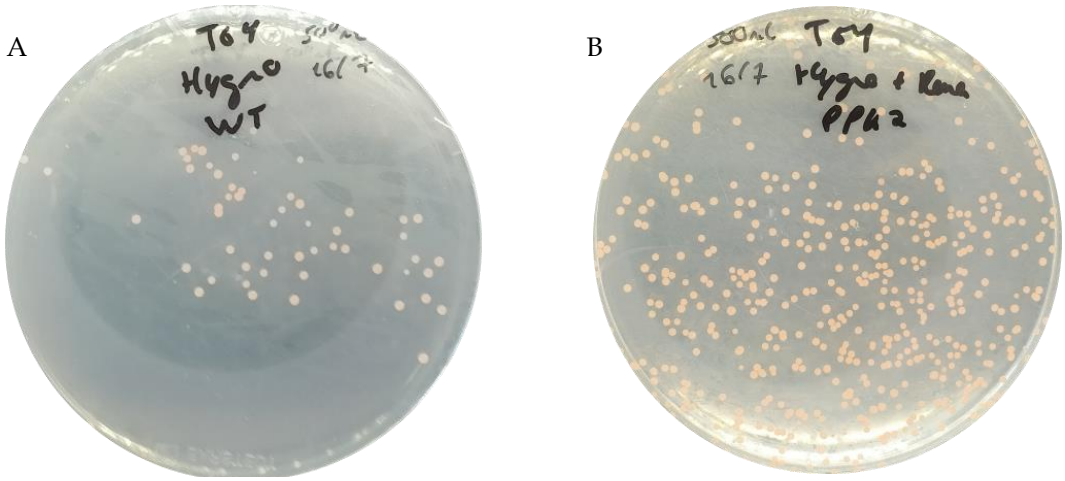


Figure 4.12 - TGY plates with the ΔPPK1 (A) and ΔPPK1/2 (B), 5 days after plating the transformation mix.

In order to confirm that the colonies that appeared on the selective plates were in fact a result of replacement of the PPK1 gene for the hygromycin resistance gene, the gDNA of both of the mutants were purified, and the entire region of the PPK1 gene (plus up (556bp) and downstream (660bp) regions) was amplified. The results showed that, Figure 4.13, in the WT genome, there was still the PPK1 gene in that region (2141bp), resulting in a fragment of around 3300bp, while from the genome of both knockout mutants the fragment amplified was around 2400bp, corresponding to the up and down sequence and the hygromycin resistance gene (1200bp), which had replaced the PPK1 gene in the genome.

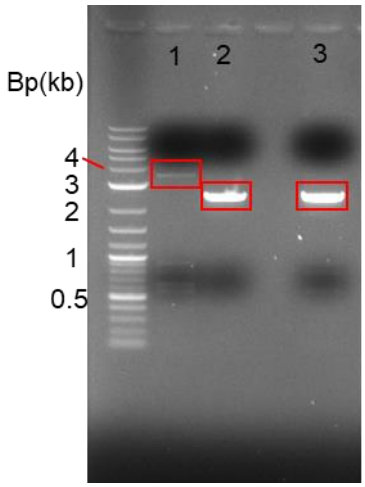


Figure 4.13 Confirmation of the PPK1 knockout mutation.
1) WT region of the PPK1 gene(2141bp) + up (556bp) + downstream (660bp) regions; 2) ΔPPK1, fragment amplified resulting in the replacement of PPK1 gene with the Hygro gene (1200bp) + up (556bp) + downstream (660bp) regions; 3) ΔPPK1/2, fragment amplified resulting in the replacement of PPK1 gene with the Hygro gene (1200bp) + up (556bp) + downstream (660bp) regions.

## 4.2 Oxidative stress and ultraviolet (UV) exposure assays

### 4.2.1 Oxidative stress exposure assays

From the oxidative stress assays, the results measured were the diameter of the inhibition areas caused by the varying concentration of either Hydrogen peroxide or Methyl viologen. As previously stated, see 1.3, Hydrogen peroxide will lead to an increase of hydroxyl radicals while Methyl viologen will generate superoxide radicals. Moreover, the interference of NaCl in the response mechanism to this stress was studied by conducting both assays in a medium with NaCl (M53) and a medium without NaCl (TGY). A decrease in the diameter of the inhibition area is the result of increased resistance while an increase in diameter means a decrease in resistance. Examples of the results, in plate form, are shown in the annexes, FigureA 4-13.

#### 4.2.1.1 EndoIII Knockout mutants

The response to two oxidative stress agents, previously described, was compared in two different media, M53 and TGY, between every EndoIII knockout mutant constructed in this work and the ΔEndoIII-1 and ΔEndoIII-3 and *Dr* WT, which were already available in our research group.

Regarding the hydrogen peroxide assays, little difference is seen between the two mediums used (Figure4.14). In M53, every knockout mutant behaves similarly, revealing a higher resistance to $H_2O_2$ than the WT bacterium at 200mM and 600mM of this compound. In the remaining concentrations the WT bacteria behaves similarly to the knockout mutants. The only other difference is at the concentration of 1M of $H_2O_2$, in which the ΔEndoIII-1/2/3 shows less resistance than the ΔEndoIII-1 and ΔEndoIII-3.

In TGY, the WT bacterium is more resistant to $H_2O_2$ at the concentration 200mM than in M53. Besides this, the behavior between the two media is similar as for the most part, every knockout mutant also behaves similarly.

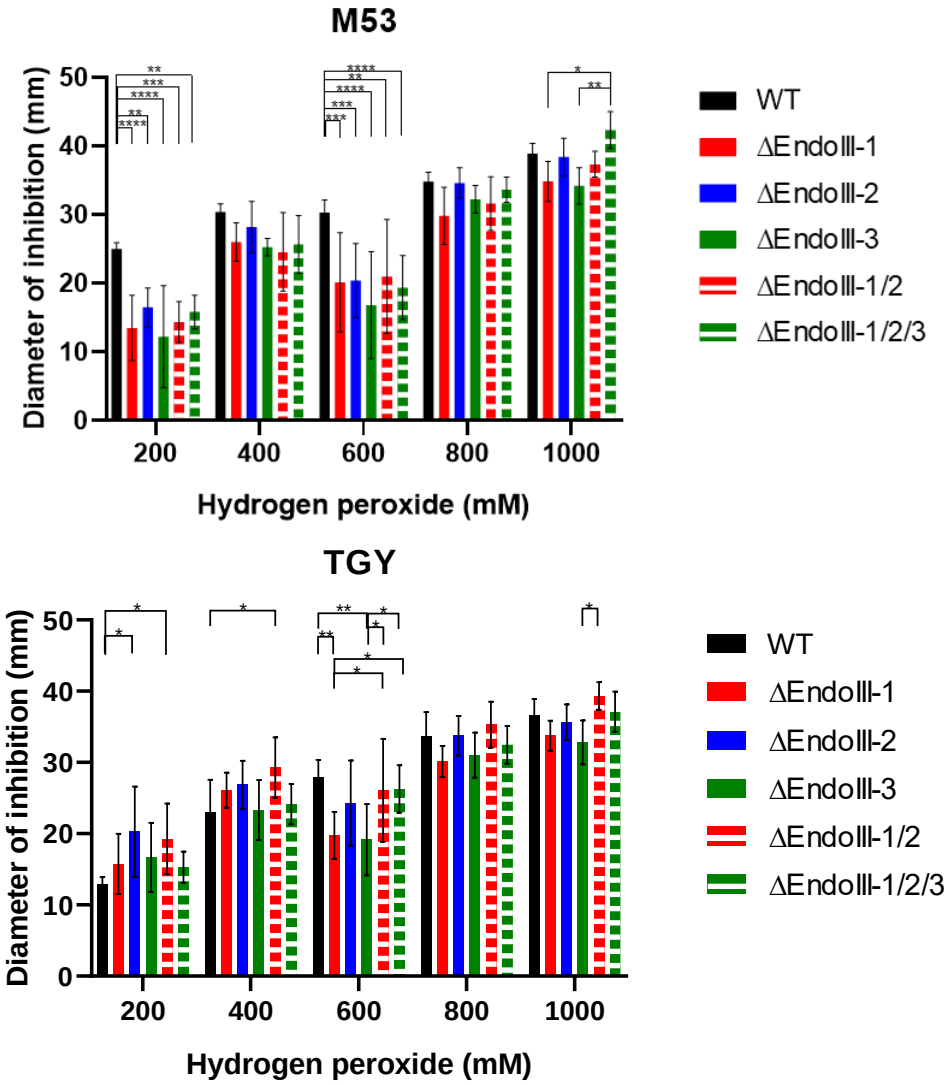


Figure 4.14 - Hydrogen peroxide assays of the EndoIII knockout mutants, in M53 and TGY.
The statistic test done was a Two-Way ANOVA and the pvalues are represented following the GP style: 0.1234 (ns), 0.0332 (*), 0.0021 (**), 0.0002 (***), <0.0001 (****).

In the methyl viologen assays, the resistance observed to this compound is completely different between the two different mediums (Figure4.15). In M53, in most of the cases, the WT bacteria is less resistant than the knockout mutants, mainly at the higher concentrations of MV, 30mM to 50mM. In these concentrations the knockout mutants behave identically while at 10mM and 20mM the ΔEndoIII-1 behaves similarly to the WT, but the other knockout mutants are much more resistant, principally the double and triple knockout mutants which at 10mM do not even form any inhibition areas. At 20mM, the ΔEndoIII-1/2 and ΔEndoIII-1/2/3 have big standard deviations due to the presence of an inhibitory effect to the cells in only some of the replicates.

Due to the great difference in resistance between the WT and the knockout mutants, in the TGY medium, the assays had to be performed with different ranges of MV concentrations. The assays with the WT strain, used a range between 2mM and 10mM while the knockout mutants' assays were between 10mM and 50mM. Because of this, the only direct comparison possible to be done is at the concentration of 10mM. At this concentration, the knockout mutants behave similarly and are more resistant than the WT bacterium. At the other concentrations the knockout mutants behave similarly with a few exceptions at 20 and 30mM.

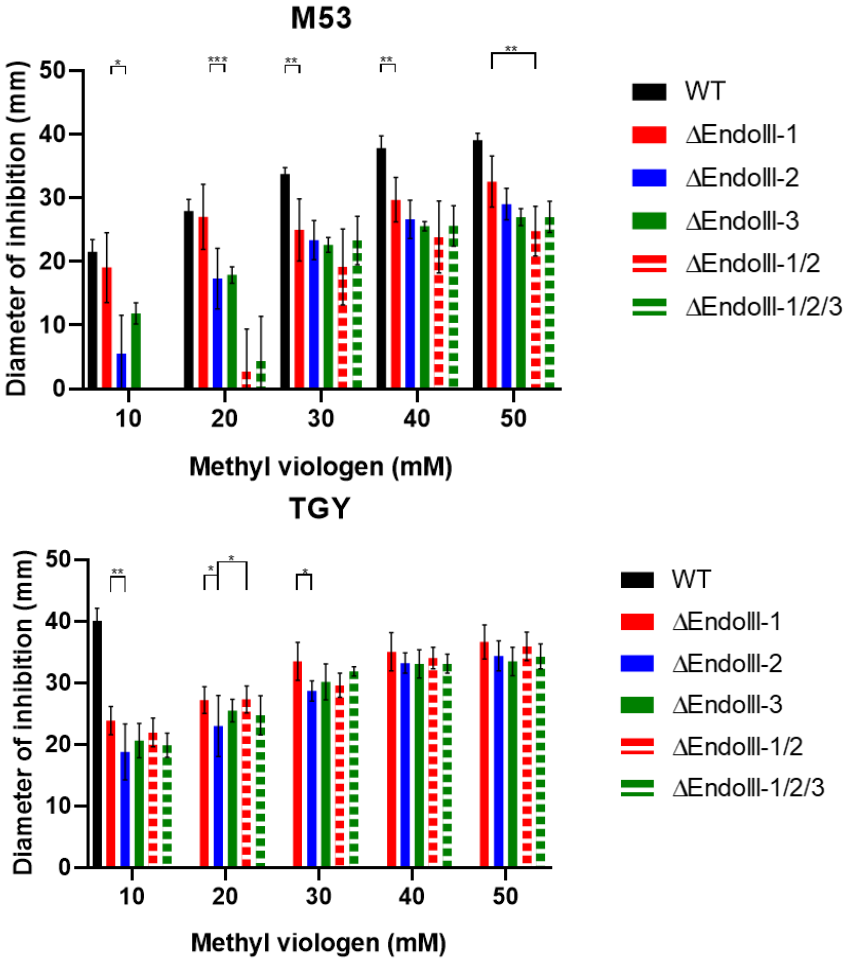


Figure 4.15 - Methyl viologen assays of the EndoIII knockout mutants, in M53 and TGY.
The statistic test done was a Two-Way ANOVA and the pvalues are represented following the GP style: 0.1234 (ns), 0.0332 (*), 0.0021 (**), 0.0002 (***), <0.0001 (****).

The results from the $H_2O_2$ assays suggested that the EndoIII proteins do not have a role in the defense against the damage done by this compound as the response, most of the time, was

similar to the WT bacteria and that no significant and constant difference was observed between the different knockout mutants.

Regarding the MV assays, the EndoIII proteins are clearly involved with a response against this damage as every knockout mutant became more resistant than the WT bacteria. This increase in resistance, might be caused by a compensatory defense mechanism of the bacteria, resulting in an overresponse of alternative or additional stress response mechanisms when compared to the WT. This response might not be sustainable for the bacteria, but more studies need to be done to prove this proposal. Despite this, no clear difference was observed between the different knockout mutants.

Additionally, there is a clear difference in response between both mediums. In M53 almost every knockout mutant presents a higher resistance than in TGY. This difference is mainly seen at the lower concentrations of MV, where, in M53, the double and triple mutants of the EndoIII proteins are not inhibited or only partially inhibited. This seems to show that M53, provides a possible resistance, at least at lower concentrations of MV. Besides the effects on the EndoIII knockout mutants, the WT bacteria also is drastically less resistant in TGY than at M53. While at 10mM of MV, in M53, the inhibition area formed has the diameter of around 20mm, in TGY this diameter doubles, to around 40mm.

#### 4.2.1.2 Dps1 Knockout mutants

The importance of Dps1 and of a possible interplay with the EndoIII-2 protein, in the response against oxidative stress was studied. For this, the ΔDps1 and ΔEndoIII-2/Dps1 were exposed to the oxidative stress assays previously described.

As it is shown in Figure4.16, in M53, both knockout mutants were more resistant to $H_2O_2$ compared to the WT. Between the knockout mutants, the only differences in behavior were at 600mM and 800mM, sharing an identical response at the remaining concentrations.

In TGY, from 200mM to 600mM the WT behaves similarly to the ΔDps1. But, at 800mM and 1M, the WT and ΔEndoIII-2/Dps1 started to share behavior, while the phenotype of the ΔDps1 showed more resistant than the other two.

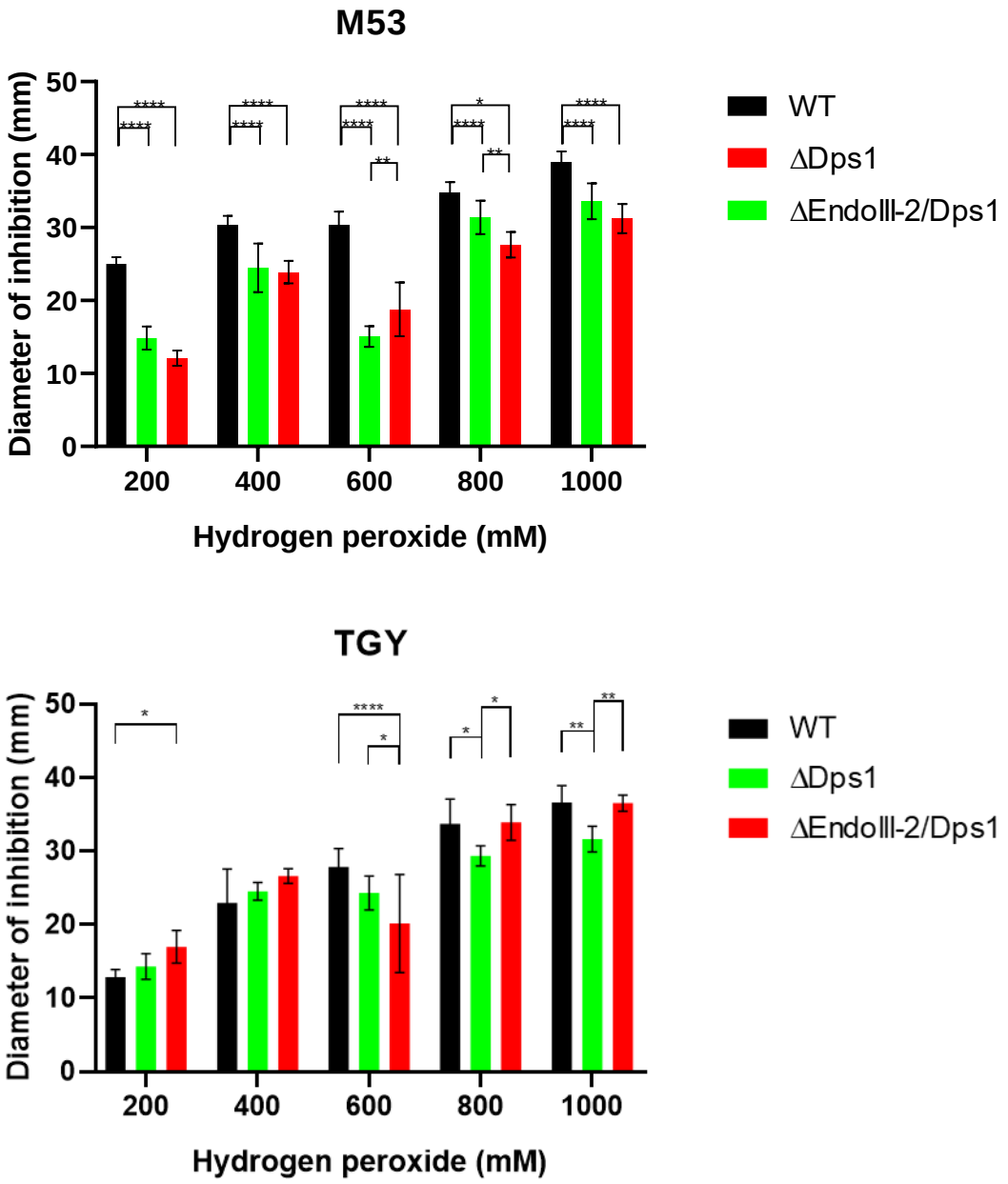


Figure 4.16 - Hydrogen peroxide assays of the Dps1 and EndoIII-2/Dps1 knockout mutants, in M53 and TGY. The statistic test done was a Two-Way ANOVA and the pvalues are represented following the GP style: 0.1234 (ns), 0.0332 (*), 0.0021 (**), 0.0002 (***), <0.0001 (****).

Regarding the MV assays (Figure4.17), in M53, both knockout mutants are more resistant than the WT bacteria, mainly the ΔEndoIII-2/Dps1 which are not inhibited at 10mM. From 20mM, the resistance is not significantly different between the two knockout mutants.

For the same reason as explained before, in TGY, the only concentration at which was possible to do a direct comparison, between the results from the knockout mutants and the WT, was

10mM. So, as expected the WT bacteria at this concentration is less resistant than both knockout mutants. The knockout mutants present the same behavior at the different concentrations of MV.

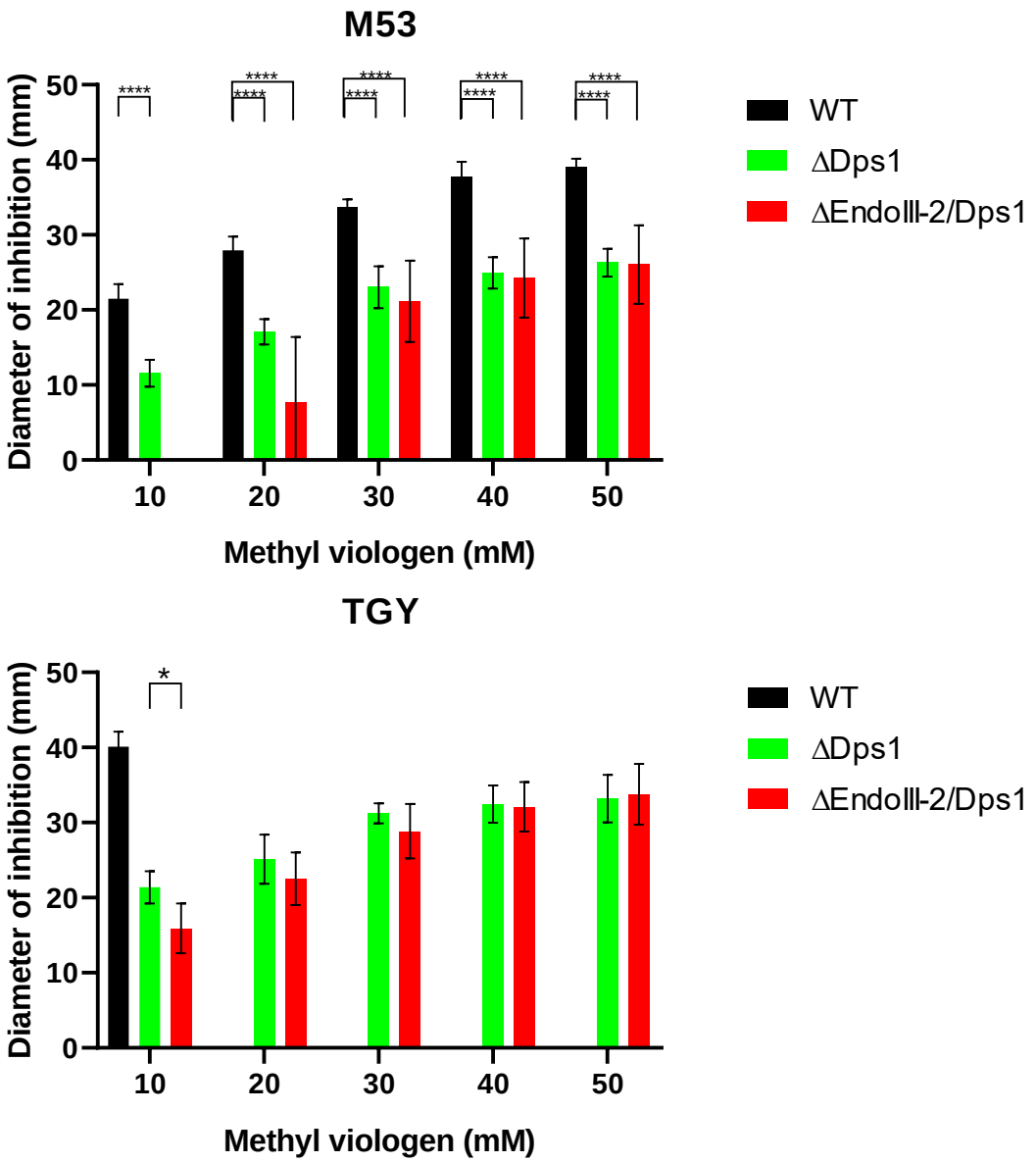


Figure 4.17 - Methyl viologen assays of the Dps1 and EndoIII-2/Dps1 knockout mutants, in M53 and TGY. The statistic test done was a Two-Way ANOVA and the pvalues are represented following the GP style: 0.1234 (ns), 0.0332 (*), 0.0021 (**), 0.0002 (***), <0.0001 (****).

From the $H_2O_2$ assays, it was possible to conclude that Dps1 might have a role in the response against this compound. In M53, both knockout mutants had a higher resistance to $H_2O_2$ and since the ΔEndoIII-2 did not behave like this, the knockout of the Dps1 protein might be the cause for this change in behavior.

Regarding the MV assays, besides EndoIII-2, Dps1 also seems to be involved in this response as the cells acquired resistance to this stress.

Again, in M53 the cells were more resistant than in TGY, at the lower concentrations of MV.

#### 4.2.1.3 PPK Knockout mutants

In order to complement these studies, we further analysed the response of knockout mutants of the polyphosphate-manganese system of the same damage. To understand the possible effects of the knockout of PPK1 and PPK2 in the response against $H_2O_2$ and MV, the same oxidative stress assays were conducted with three knockout mutants (ΔPPK1, ΔPPK2 and ΔPPK1/2). These assays were only conducted in M53, due to it being the medium in which the knockout mutants presented a more significant response.

These results (Figure4.18) presented a clear increase of resistance in the ΔPPK2, in comparison with WT and even the other knockout mutants. The ΔPPK1 and ΔPPK1/2 have a similar behavior as the WT, except for the double knockout mutant at 200mM.

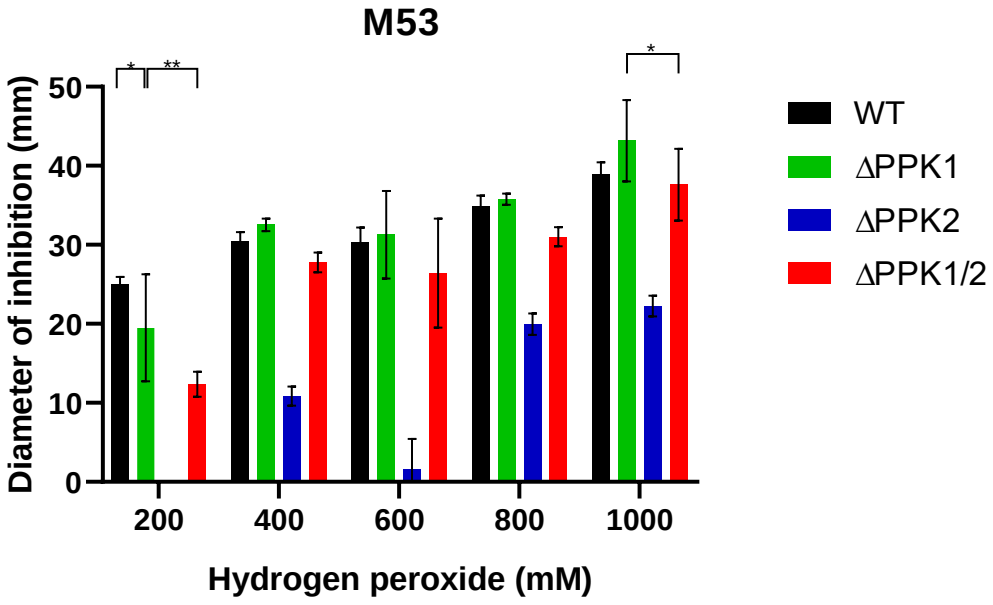


Figure 4.18 - Hydrogen peroxide assays of the PPK knockout mutants, in M53.
The statistic test done was a Two-Way ANOVA and the pvalues are represented following the GP style: 0.1234 (ns), 0.0332 (*), 0.0021 (**), 0.0002 (***), <0.0001 (****).

The MV assays (Figure4.19) clearly show that PPK2 has a role in the response against MV and its absence is sufficient for the bacteria to acquire resistance as the behavior of the ΔPPK2 is identical to ΔPPK1/2.

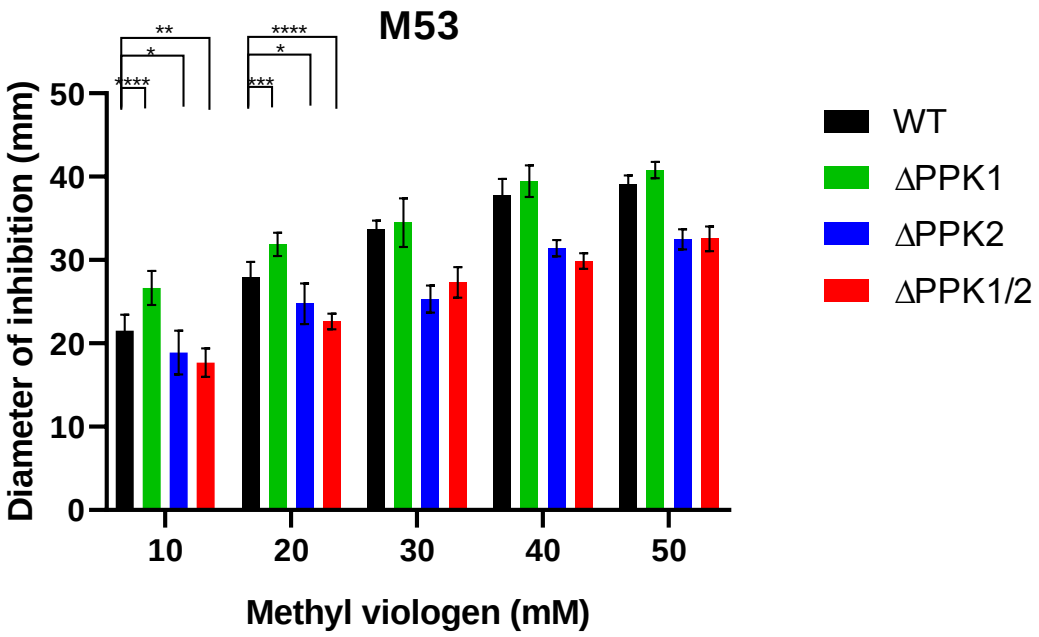


Figure 4.19 - Methyl viologen assays of the PPK knockout mutants, in M53.
The statistic test done was a Two-Way ANOVA and the pvalues are represented following the GP style: 0.1234 (ns), 0.0332 (*), 0.0021 (**), 0.0002 (***), <0.0001 (****).

From the $H_2O_2$ assays, it appears that in the absence of both PPK proteins, a compensatory mechanism that allows the double knockout mutant to behave similarly as the WT, while the ΔPPK2 has acquired resistance.

Regarding the MV assays, PPK2 reveals a very important role in the response against the stress caused by MV.

### 4.2.2 Ultraviolet exposure assays

The same knockout mutants used in the oxidative stress assays were also exposed to different doses of UV-C radiation. The results here presented were obtained by calculating the colony forming units (CFU) in different plates. The average of CFU between the replicates was done and this result was divided by the CFU calculated in the control plate, which was exposed to 0s of UV-C radiation. These ratios were then transformed to the logarithmic scale. The fluence calculations were previously explained in 3.2.1. Examples of the results, in plate form, are shown in the annexes, FigureA 4-13.

To guarantee that the UV-C radiation did not degrade the antibiotics, causing deleterious effects to the growths, a control experiment was conducted. Before pipetting the 5µL drops to the plates, plates with the three antibiotics were irradiated for 60 seconds with UV-C radiation. The drops were then pipetted and the results from these plates were compared with the plates with no exposure to UV-C radiation (FigureA 14). This control experiment revealed that no difference was observed between the plates which were exposed to UV-C radiation before the addition of the 5 µL and the ones that were not exposed at all with the UV-C radiation.

#### 4.2.2.1 EndoIII Knockout mutants

The role of the EndoIII proteins in the response against the UV-C radiation was studied by exposing knockout mutants of the EndoIII proteins to ultraviolet radiation (254nm) following the protocol explained in 3.2.1.

In M53, the single and double knockout mutants are more resistant to the UV-C radiation effects, than the WT bacteria (Figure4.20). Only the triple knockout mutant was clearly less resistant than the WT. This might mean that the absence of the three EndoIII proteins causes the cells to lose resistance while in the knockout of just one or two EndoIII-3 proteins, a compensatory mechanism is activated, in the response of an extreme condition, probably by overexpressing the remaining EndoIII proteins.

In TGY, every knockout mutant shares the same behavior even though ΔEndoIII-1 and ΔEndoIII-3 seem to be more resistant, to the UV-C radiation, than the WT at the lower dosages of UV-C radiation.

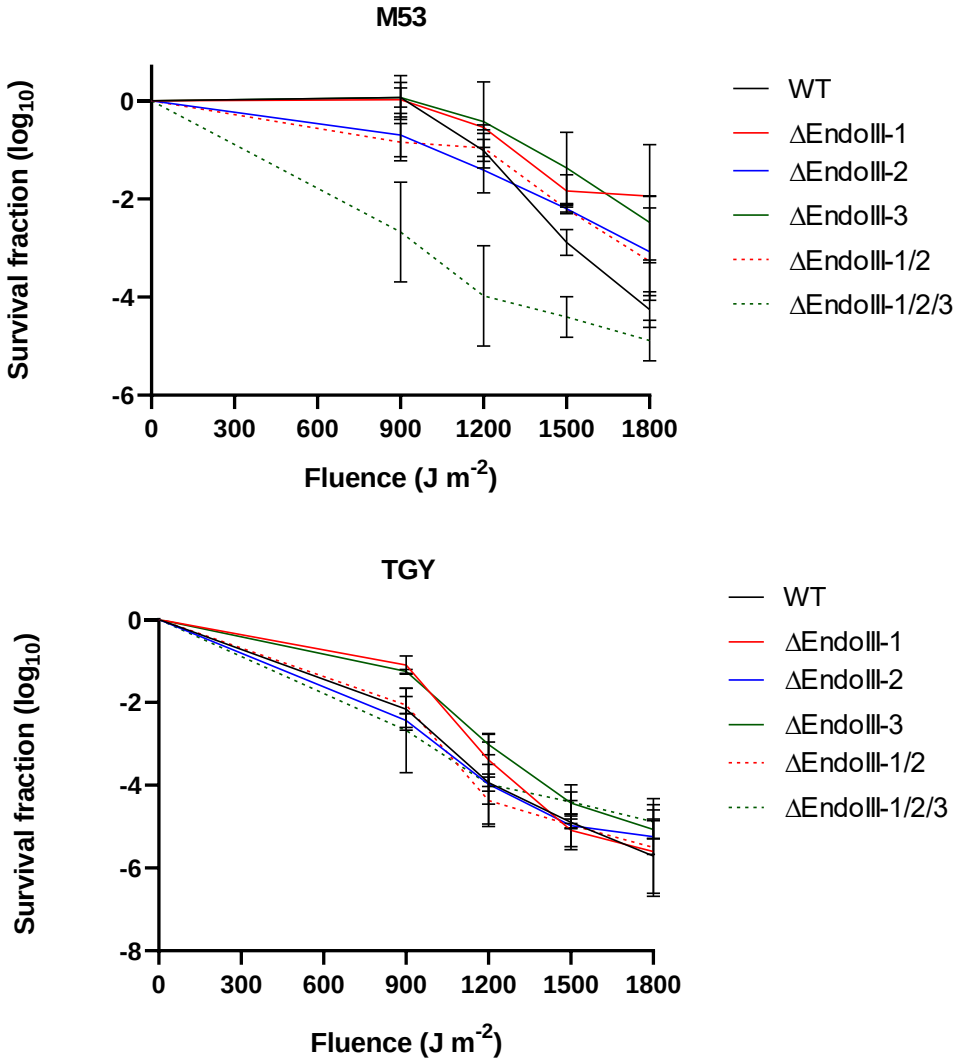


Figure 4.20 - UV-C assays of the EndoIII knockout mutants, in M53 and TGY.

The assays conducted in M53, suggested that the EndoIII proteins have a role in the defense against the exposure to UV-C radiation. In contrast, this does not seem to be the case in TGY as the knockout mutants behave similar to the WT.

#### 4.2.2.2 Dps1 Knockout mutants

Interestingly, the response between the ΔDps1 and ΔEndoIII-2/Dps1 were completely different depending on the medium, Figure4.21. In M53, the ΔDps1 and ΔEndoIII-2/Dps1 became more resistant than the WT bacteria but had a similar behavior between them.

In TGY, both knockout mutants became less resistant than the WT bacteria, but this time they behaved differently. The double knockout mutant was the least resistant, not showing any viability at 1500J/m$^2$.

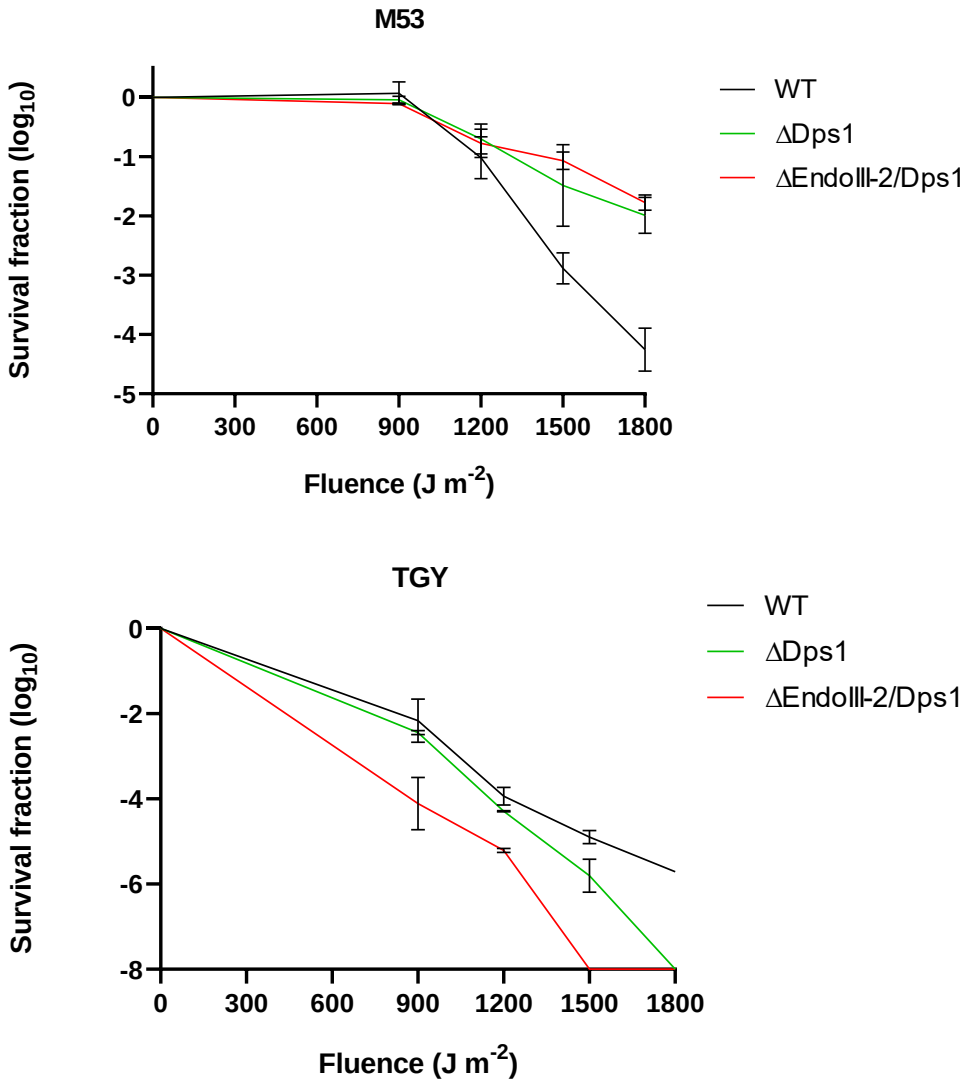


Figure 4.21 - UV-C assays of the Dps1 and EndoIII-2/Dps1 knockout mutants, in M53 and TGY.

This clearly shows that these two proteins are involved in the response against UV-C radiation damage and possibly are even cooperatively working in the TGY medium.

#### 4.2.2.3 PPK Knockout mutants

The PPK knockout mutants were exposed as well to the same UV-C assays, but as the oxidative stress assays, the experiment was only done in M53 (Figure4.22). The ΔPPK1 behaves similarly as the WT bacteria. On the other hand, both the ΔPPK2 and the ΔPPK1/2 have more resistance to the UV-C damage.

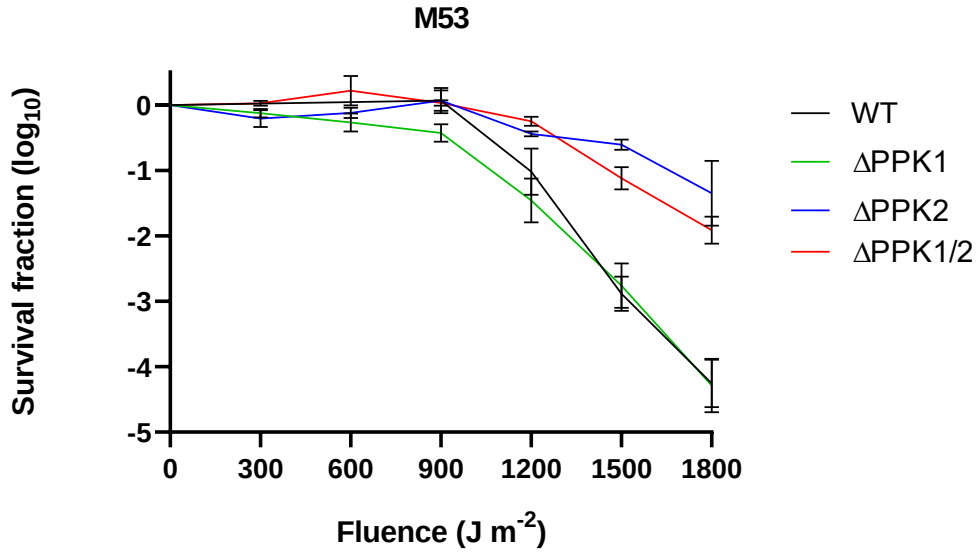


Figure 4.22 - UV-C assays of the PPK knockout mutants, in M53.

These results might mean that PPK1 is not involved in this response while PPK2 is deeply connected with this response.

## 4.3 EndoIII-2 mutation

### 4.3.1 Generation and confirmation of the EndoIII-2 mutant

To understand the molecular mechanisms of EndoIII-2, the determination of its crystal structure is essential. Despite several attempts, no crystals have been obtained of EndoIII-2. In order to try to obtain protein crystals, changes on the surface charges, are sometimes required, and are done by either adding agents, which might be protein ligands, to promote crystallization, or doing point mutations in the protein surface[73]. In this work, a single amino acid substitution (A61R) has been introduced which aim was to alter the surface charge of the proteins, by substituting a hydrophobic side chain residue for a positive side chain residue. The protocol for the generation of the single mutant was described in 3.3.

As explained in 3.4, the mutation was introduced into the gene encoding for EndoIII2 by using the NZYtech mutagenesis kit, and the resulting plasmid was then used to transform *E. coli* expression strain BL21(DE3)pLysS. The transformation mix was plated in LB solid medium, with chloramphenicol (35µg/mL) and ampicillin (100µg/mL). The reaction was incubated overnight at 37ºC. On the next day, colonies were observed on the plate, as seen in Figure4.23. To confirm that the desired mutation had been introduced into the EndoIII-2 gene, pDNA was purified from LB growths of two colonies. Each sample of pDNA was sent to sequencing through the Eurofins platform. From each pDNA sample, two different samples were sent, one with the forward primer and one with the reverse primer.

Figure 4.23 - LB plate with the overnight transformants.
The colonies which grew on the plate were BL21(DE3) pLysS after transformation with a pDest14 with the EndoIII-2 gene.

The sequencing results were analyzed using the Bioedit sequence alignment software[74] One of the 4 sequences received, did not give any information as the sequence was too small (clone 1 with the forward primer). The sequence of the remaining three fragments was analyzed and edited manually using the sequencing chromatograms as some parts of the sequence seemed to be different from the template. After correcting the sequence, it was translated into protein sequence using the EsPript 3 software[75], Figure4.24. In these sequences two amino acid changes are observed. One was the result of the target mutation, from an alanine to an arginine in position 61, and the other, from a valine to an arginine in position 1, which had been generated prior to this work, in order to allow the TEV to cleave the His tag from the protein. The alignment of the nucleotide sequence between the clones and the EndoIII-2 gene is shown in FigureA 15.

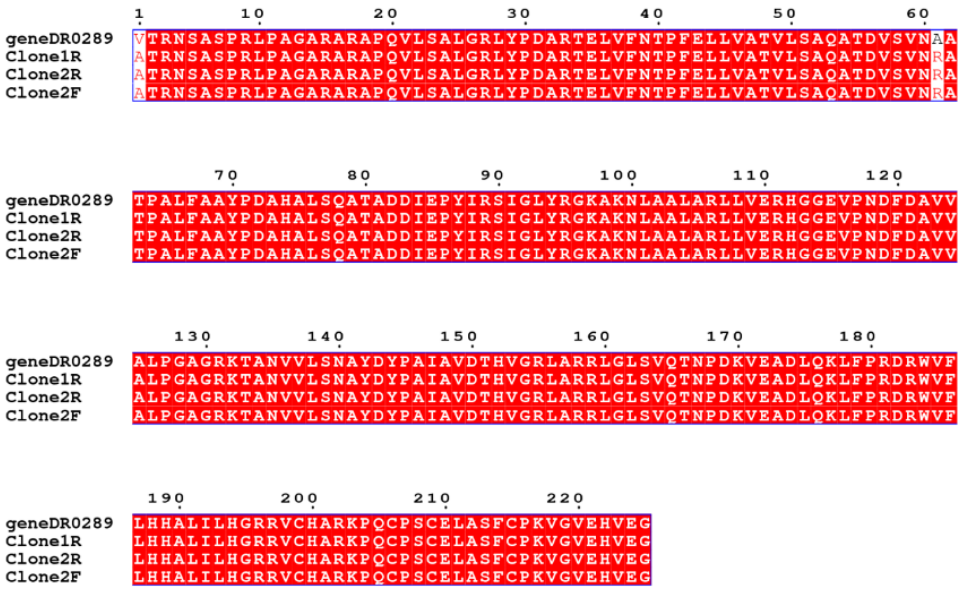


Figure 4.24 - Protein sequencing results of the EndoIII-2 inserted into a pDest14 and compared with the WT sequence. The mutations are highlighted in white.

### 4.3.2 Expression, purification and crystallization of EndoIII-2A61R

A transformation of BL21(DE3)pLysS was performed, as explained in 3.4.1, with the clone 1 plasmid. After that, two one-liter growths were done and the resulting pellets, from the harvest of the cells, weighed around 6 grams.

One of the pellets was then resuspended (see in 3.4.2) in the extraction buffer, the cells were disrupted through three cycles of freeze and thaw, followed by a centrifugation (39,191 xg in Avanti J26 XPI with JA25.50 rotor) in order to clarify the extract for purification. From that, the sample was injected into a His Trap column and resulted in one clear peak at around 50% Buffer B as seen in Figure4.25. The iron-sulfur cluster gives the protein a yellowish color, allowing to "see" the protein in the collection tubes throughout the purification steps.

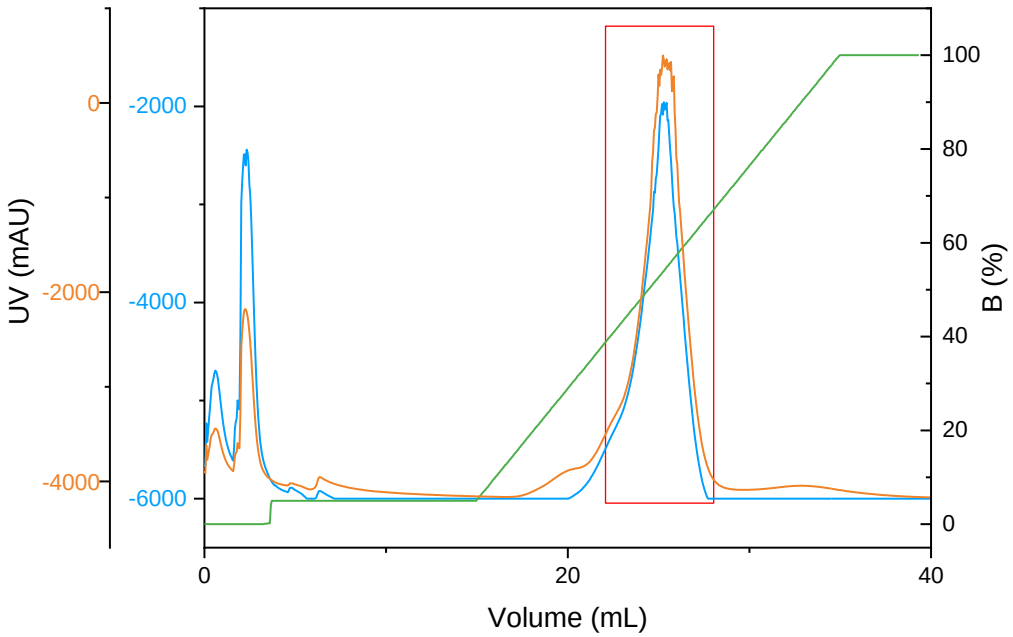


Figure 4.25 - Chromatogram of a His Trap column of 1mL of the A61R EndoIII-2 sample.
In blue is the absorbance at 254nm; In orange is the absorbance at 280nm; In green is the percentage of Buffer B.

The fractions corresponding to that peak, were pooled and injected into a Heparin column after removing the Imidazole by desalting in a PD10 column. This run resulted in a sharp peak, corresponding to the D5 to E1 fractions, at around 30% of Buffer B, as seen in Figure4.26.

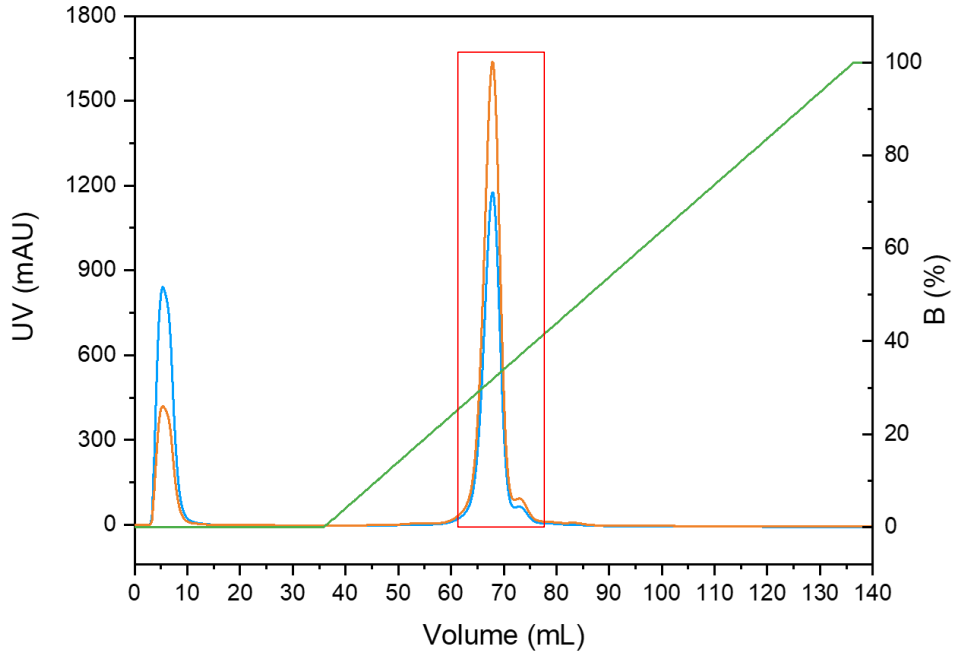


Figure 4.26 - Chromatogram of a Heparin column of 5mL of the A61R EndoIII-2 sample.
In blue is the absorbance at 254nm; In orange is the absorbance at 280nm; In green is the percentage of Buffer B.

The fractions corresponding to this peak, were analyzed in a 12.5% SDS-PAGE. The label given to the fractions is from the well, of the 96-well plates, in which the samples were collected. From this gel (Figure4.27) the samples appeared to be pure, being the EndoIII-2 band (26 kDa) the only band visible in every well.

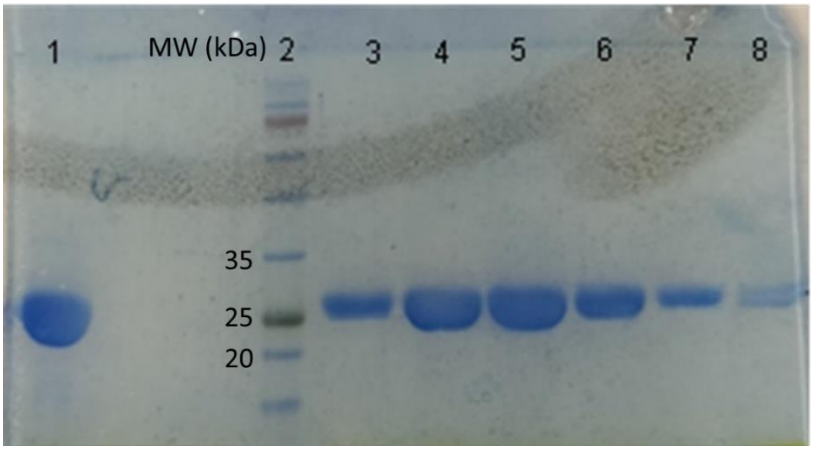


1 – EndoIII-2 control

2 – NZYcolour Protein Marker II

3 – D5

4 - D4

5 - D3

6 - D2

7 – D1

Figure 4.27 - 12.5% SDS-PAGE with the samples corresponding to the EndoIII-2 peak, purified from the heparin column.

The 6 fractions were pooled and concentrated to around 18mg/mL. With this sample, 3 crystallization screens were done, as explained in 3.4.4. Unfortunately, no crystals were observed in any of the screens, but the screens are being closely monitored in case of the appearance of a crystal.

In the JCSG+ crystallization screen, around 70-80% of the drops presented protein precipitates. Examples of drops with protein precipitates are shown in Figure4.28-A. The Index crystallization screen had around 40% of protein precipitates and the Morpheus only around 10-20%. Examples of clear drops are shown in Figure4.28-B.

A wide variety in the appearance of the drops (presence of protein precipitates and clear drops) is important in a crystallization screen as it means that the concentration of the protein being used is sufficient for the crystallization to occur. If only drops with protein precipitates were observed, the protein concentration used was too high. If only clear drops were seen, probably the protein would have to be concentrated further.

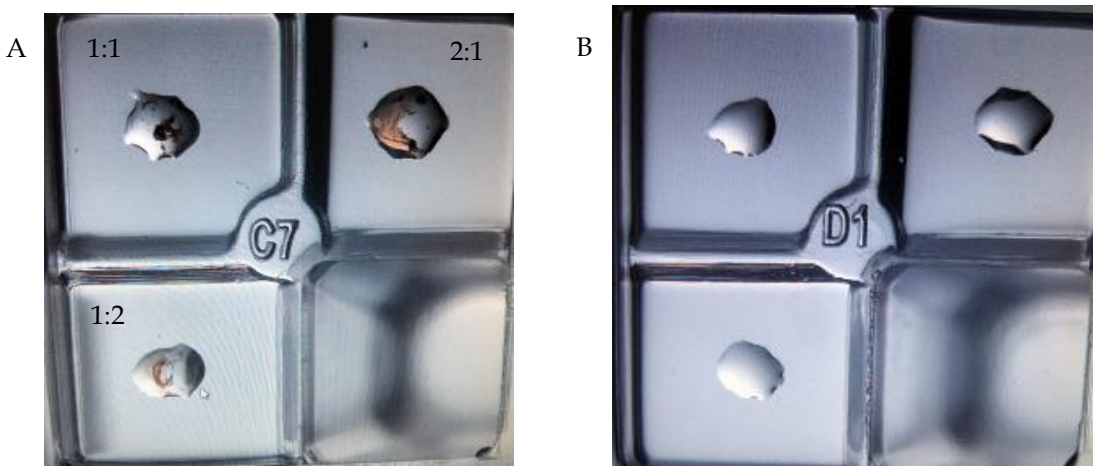

Figure 4.28 - Crystallization drops examples of the crystallization screens.
The ratios presented in the image A correspond to the protein: crystallization solution ratio.

For future work, the possible route to take would be to try other crystallization screens. Additionally, despite the protein being pure, an additional purification step, such as a molecular filtration chromatography, could be done to improve protein stability, possibly promoting crystallization. Furthermore, as EndoIII-2 is able to bind to DNA, crystallization with DNA could be attempted.

# 5

# DISCUSSION AND GENERAL CONCLUSION

We were able to establish a protocol for generation of knock out mutants of *D. radiodurans* which is easy and reliable. The method is based on the principles of Fusion PCR and homologous recombination (HR). It includes the generation of a linear PCR fragment with a selection marker (antibiotic resistance gene) flanked by genome specific sequences (upstream and downstream) of the target knock out gene, which will be replaced by the selection marker by HR upon transformation. For this, all that is needed, is to design 6 specific primers, to amplify and ligate the three fragments, besides having available standard PCR equipment and reagents, agarose gel electrophoresis equipment, a gel extraction kit and equipment for growth of bacteria.

The different knockout mutants generated were constructed with the aim of studying 3 distinct groups of proteins which play different roles in the cells upon exposure to genotoxic stress (protection or repair). Dps proteins are involved in protecting the DNA from suffering extensive damage and are also involved in metal homeostasis ($Mn^{2+}$ and $Fe^{2+}$) while EndoIII proteins removes oxidation damaged bases in DNA in the BER pathway. The PPK proteins are essential for the metabolism of PolyP which are involved in several pathways to guarantee the cell's viability.

Throughout the experimental work, in the oxidative stress and UV-C radiation assays, three types of stress conditions were used: Methyl viologen or paraquat, which generates superoxide radicals; Hydrogen peroxide which alter protein conformation and, through the Fenton reaction, is converted to hydroxyl radicals[76]; and UV-C radiation which besides being capable of generating DSB in the DNA also leads to the formation of ROS, such as singlet oxygen.

Besides this, two different media were used in order to study the influence of NaCl, on the response mechanisms to different stress conditions, as M53 contained NaCl while TGY did not.

There were some very interesting results, ranging from no difference between the knockout mutants' and the WT as observed in the $H_2O_2$ assays, to clear differences as in the MV assays, except for the ΔPPK1. Regarding the UV-C assays, the results seemed to depend on the media and only the triple knockout mutant of the EndoIII became less resistant to this stress. All of these results are summarised in Table5.1.

Table 5.1 Main results of the oxidative stress and UV-C assays.
The results presented are related to the resistance of the knockout mutants in comparison with the WT. (+) more resistant: (0) same resistance; (-) less resistant. The amount of (-) or (+) relates to the difference between the resistance observed in WT and the knockout mutants.

| | | M53 | | | TGY | | |
|---|---|---|---|---|---|---|---|
| | | $H_2O_2$ | MV | UV-C | $H_2O_2$ | MV | UV-C |
| DNA repair system | ΔEndoIII-1 | 0 | ++ | ++ | 0 | +++ | 0 |
| | ΔEndoIII-2 | 0 | ++ | + | 0 | +++ | 0 |
| | ΔEndoIII-3 | 0 | ++ | ++ | 0 | +++ | 0 |
| | ΔEndoIII-1/ EndoIII-2 | 0 | ++ | + | 0 | +++ | 0 |
| | ΔEndoIII-1/ EndoIII-2/ EndoIII-3 | 0 | ++ | -- | 0 | +++ | 0 |
| DNA protection system and metal homeostasis | ΔDps1 | + | + | + | 0 | +++ | - |
| | ΔEndoIII-2/Dps1 | + | + | + | 0 | +++ | -- |
| Pi-Manganese system | ΔPPK1 | 0 | 0 | 0 | | | |
| | ΔPPK2 | ++ | + | +++ | | | |
| | ΔPPK1/PPK2 | 0 | + | +++ | | | |

Regarding the EndoIII proteins it was observed that the knockout mutants, in the $H_2O_2$ assays, had a similar behavior to the WT. These results were not media dependent as they were the same in both media. This shows that these proteins are not important in the response against $H_2O_2$ and that NaCl does not play a part in this response.

The methyl viologen assays revealed a role of these proteins in the response against this compound. These results showed an increase of resistance of the knockout mutants when compared with the WT. Additionally the increase of resistance was more severe in the absence of NaCl. The results collected from the knockout mutants' assays were, for the most part similar, except for the 10mM and 20mM of MV, in the presence of NaCl, in which EndoIII-1 behaves similar to the WT, the EndoIII-2 and EndoIII-3 show an intermediate gain of resistance and the double and triple mutant present almost no viability.

The fact that the knockout mutants of EndoIII respond similarly at higher concentrations of MV, while differently at the lower concentrations (10 and 20mM), might mean that the cells possess a threshold for the compounds that is generated in the cells upon exposure to MV. It is known from the literature that superoxide radicals can cause the loss of function to iron sulfur clusters[77]. In this case, it may mean that when that concentration is reached, the iron sulfur proteins are inactivated, resulting in all the knockouts having the same resistance. However, more studies will be needed in order to confirm this proposal.

The UV-C assays showed a clear influence of NaCl. While in TGY these proteins appeared to have no function in the response against UV-C radiation damage, in M53 most of the knockout mutants became more resistant than the WT, except for the triple mutant which became less resistant. This might mean that, in M53, the single and double knockout mutants are able to upregulate other defense pathways to withstand the stress resulting in the organism becoming even more resistant than the WT bacterium. But, once the three EndoIII proteins are absent from the cell, it is not able to upregulate other defense mechanisms, resulting in a decrease in resistance.

The Dps1 and the EndoIII-2-Dps1 knockout mutants in M53, in the $H_2O_2$ assays, were more resistant than the WT. In TGY, both knockout mutants responded similarly to the WT. In the MV assays, the response of the knockout mutants showed a more resistant behavior to this compound than the WT. The UV-C assays revealed again that the response to the stress was medium dependent as the assays conducted in M53 showed that both knockout mutants

became more resistant, while in TGY they became less resistant. Additionally, while in M53 the knockout mutants respond similarly, in TGY the double knockout mutant is more sensitive than the single knockout mutant of Dps1. This might mean that Dps1 and EndoIII-2 have an interplay in the response against UV-C radiation in TGY.

The PPK knockout mutants (ΔPPK1, ΔPPK2 and ΔPPK1/2), in the $H_2O_2$ assays, behaved differently amongst them. ΔPPK1 and ΔPPK1/2 behaved identically to the WT, while ΔPPK2 was much more resistant. This means that PPK1 is not involved in the response against $H_2O_2$ damage. On the contrary, PPK2 has a key role in this response. The fact that the double knockout mutant behaved as the WT might mean that a compensatory mechanism is activated when both PPK proteins are absent, allowing the cells to have the same response as the WT. But further studies need to be performed in order to confirm this proposal. In the MV assays, ΔPPK1 showed the same response as the WT but the exposure to this stress caused ΔPPK2 and ΔPPK1/2 to have similar responses, meaning that under MV damage the compensatory mechanism is not observed. In the UV-C assays, ΔPPK1 had the same response as the WT while both other knockout mutants were more resistant, which, again, means that PPK2 is deeply involved in this response. The difference in response observed between M53 and TGY is proposed to be due to the different behavior presented by *Dr* cells, as it has been previously reported[78]. In M53, cells form agglomerates while in TGY they do not. This behavior change might be the reason to the fact that cells in M53 are more resistant to external agents than cells in TGY.

A possible explanation for the increase of resistance of some knockout mutants in some stress conditions is the previously observed delocalization of metals throughout the cells, in the knockout mutant of Dps1[20]. Those metals and polyphosphate complexes, in control conditions are localized in electron dense granules. But in the case of the ΔDps1 these complexes are spread throughout the cells' cytosol. This might cause the cells to react better to a severe stress, but we think that this response might not be sustainable if another extreme stress conditions were to be exposed to these knockout mutants, but more studies need to be performed in order to be able to confirm this proposal. Additionally, the knockout mutants grew to higher OD600nm values than the WT (Figures A1 and A2). This may indicate that also other compensatory metabolic processes become activated, resulting in higher resistances to the stress than the WT.

Regarding the crystallization of the mutated EndoIII-2, no crystals were obtained, confirming the difficulty of crystallizing the EndoIII-2 protein. This experiment showed that the mutation done, alone, was not enough to promote crystallization. But we propose that a step in the right direction has been taken, as in the past, using the native protein, the percentage of clear drops in the crystallization plates was much higher (oral communication from Elin Moe) in comparison with the percentages obtained in this work. For future work, other crystallization screens could be experimented, like the Structure 1&2. Other mutations might also be required to facilitate crystallization of EndoIII-2.

# 6
# REFERENCES


1. Lourenço, J. M. NOVA Thesis Word Template. https://www.fct.unl.pt/estudante/informacao-academica/teses-e-dissertacoes.
2. Lim, S., Jung, J. H., Blanchard, L. & De Groot, A. Conservation and diversity of radiation and oxidative stress resistance mechanisms in Deinococcus species. *FEMS Microbiol. Rev.* **43**, 19–52 (2019).
3. Lysenko, V. S. *et al.* Separation and mass spectrometry identification of carotenoid complex from radioresistant bacteria Deinococcus radiodurans. *J. Anal. Chem.* **66**, 1281–1284 (2011).
4. Krisko, A. & Radman, M. Biology of extreme radiation resistance: The way of Deinococcus radiodurans. *Cold Spring Harb. Perspect. Biol.* **5**, (2013).
5. Nitzan, Y. & Ashkenazi, H. Photoinactivation of Deinococcus radiodurans: An unusual gram-positive microorganism. *Photochem. Photobiol.* **69**, 505–510 (1999).
6. Levin-Zaidman, S. *et al.* Ringlike structure of the Deinococcus radiodurans genome: A key to radioresistance? *Science (80-. ).* **299**, 254–256 (2003).
7. White, O. *et al.* Genome sequence of the radioresistant bacterium Deinococcus radiodurans R1. *Science (80-. ).* **286**, 1571–1577 (1999).
8. Minton, K. W. Repair of ionizing-radiation damage in the radiation resistant bacterium Deinococcus radiodurans. *Mutat. Res. - DNA Repair* **363**, 1–7 (1996).
9. Battista, J. R. Against all odds: The survival strategies of Deinococcus radiodurans. *Annu. Rev. Microbiol.* **51**, 203–224 (1997).
10. Ghosal, D. *et al.* How radiation kills cells: Survival of Deinococcus radiodurans and Shewanella oneidensis under oxidative stress. *FEMS Microbiol. Rev.* **29**, 361–375 (2005).
11. Daly, M. J. Accumulation of Mn(II) in Deinococcus radiodurans Facilitates Gamma-Radiation Resistance. *Science (80-. ).* **306**, 1025–1028 (2004).
12. Blasius, M., Sommer, S. & Hübscher, U. Deinococcus radiodurans: What belongs to the survival kit? *Crit. Rev. Biochem. Mol. Biol.* **43**, 221–238 (2008).
13. Hansen, M. T. Multiplicity of genome equivalents in the radiation resistant bacterium Micrococcus radiodurans. *J. Bacteriol.* **134**, 71–75 (1978).
14. Heinloth, A. N. *et al.* Identification of distinct and common gene expression changes after oxidative stress and gamma and ultraviolet radiation. *Mol. Carcinog.* **37**, 65–82

(2003).

15. Sukhi, S. S., Shashidhar, R., Kumar, S. A. & Bandekar, J. R. Radiation resistance of Deinococcus radiodurans R1 with respect to growth phase. *FEMS Microbiol. Lett.* **297**, 49–53 (2009).

16. Cox, M. M., Keck, J. L. & Battista, J. R. Rising from the ashes: DNA repair in Deinococcus radiodurans. *PLoS Genet.* **6**, 1–2 (2010).

17. Qi, H. zhou *et al.* Antioxidative system of Deinococcus radiodurans. *Res. Microbiol.* **171**, 45–54 (2020).

18. Slade, D. & Radman, M. *Oxidative Stress Resistance in Deinococcus radiodurans . Microbiology and Molecular Biology Reviews* vol. 75 (2011).

19. Daly, M. J. A new perspective on radiation resistance based on. *Nat. Rev. Microbiol.* **7**, 16–18 (2009).

20. Santos, S. P. *et al.* The interplay between Mn and Fe in Deinococcus radiodurans triggers cellular protection during paraquat-induced oxidative stress. *Sci. Rep.* **9**, 1–12 (2019).

21. Lushchak, V. I. Oxidative stress and mechanisms of protection against it in bacteria. *Biochem.* **66**, 476–489 (2001).

22. Wijeratne, S. S. K., Cuppett, S. L. & Schlegel, V. Hydrogen peroxide induced oxidative stress damage and antioxidant enzyme response in Caco-2 human colon cells. *J. Agric. Food Chem.* **53**, 8768–8774 (2005).

23. Ahmad, P., Jaleel, C. A., Azooz, M. M. & Nabi, G. Generation of ROS and non-enzymatic antioxidants during abiotic stress in plants. *Bot. Res. Int.* **2**, 11–20 (2009).

24. Aysla Costa De Oliveira, M., D'Epifanio, A., Ohnuki, H. & Mecheri, B. Platinum group metal-free catalysts for oxygen reduction reaction: Applications in microbial fuel cells. *Catalysts* **10**, 1–21 (2020).

25. Van Acker, H. & Coenye, T. The Role of Reactive Oxygen Species in Antibiotic-Mediated Killing of Bacteria. *Trends Microbiol.* **25**, 456–466 (2017).

26. Cornelis, P., Wei, Q., Andrews, S. C. & Vinckx, T. Iron homeostasis and management of oxidative stress response in bacteria. *Metallomics* **3**, 540–549 (2011).

27. Cabiscol, E., Tamarit, J. & Ros, J. Oxidative stress in bacteria and protein damage by reactive oxygen species. *Int. Microbiol.* **3**, 3–8 (2000).

28. Centennial, T. H. E., The, O. F. & Reaction, F. 1-s2.0-089158499390168T-main.pdf. **15**, 645–651 (1993).

29. Picardo, M. & Dell'Anna, M. L. Oxidative stress. *Vitiligo* 231–237 (2010) doi:10.1007/978-3-540-69361-1_27.

30. Breithaupt, J. Summary Review of Available Literature for Hydrogen Peroxide and Peroxyacetic Acid for New Use for New Use to Treat Wastewater. 8–11 at (2007).

31. Ishii, N. *et al.* A methyl viologen-sensitive mutant of the nematode Caenorhabditis elegans. *Mutat. Res. DNAging* **237**, 165–171 (1990).

32. Lascano, R. *et al.* Paraquat: An Oxidative Stress Inducer. *Herbic. - Prop. Synth. Control Weeds* (2012) doi:10.5772/32590.

33. Hassan, H. M. & Fridovich, I. Paraquat and Escherichia coli. Mechanism of production of extracellular superoxide radical. *J. Biol. Chem.* **254**, 10846–10852 (1979).

34. Landrum, J. T. *Carotenoids and human health*. *Reactive Oxygen and Nitrogen Species in Biological Systems: Reactions and Regulation by Carotenoids* (2013). doi:10.1007/978-1-62703-203-2.

35. Nyska, R. K. and A. Oxidation of Biological Systems: Oxidative Stress Phenomena, Antioxidants, Redox Reactions, and Methods for Their Quantification. *Toxic Pathol.* (2002) doi:10.1080/0192623029016672.

36. Blaustein, A. R. & Searle, C. Ultraviolet Radiation. *Encycl. Biodivers. Second Ed.* 296–303 (2013) doi:10.1016/B978-0-12-384719-5.00147-7.

37. Urban, L., Charles, F., de Miranda, M. R. A. & Aarrouf, J. Understanding the physiological effects of UV-C light and exploiting its agronomic potential before and after harvest. *Plant Physiol. Biochem.* **105**, 1–11 (2016).

38. Fan, X., Huang, R. & Chen, H. Application of ultraviolet C technology for surface decontamination of fresh produce. *Trends Food Sci. Technol.* **70**, 9–19 (2017).

39. Bankovska, S., Konstantinovs, A., Bakovskis, P., Gaivoronskis, A. & Bankovskis, V. Germicidal and Antiviral decontamination of air by UV irradiation and UV recirculator method. 1–8 (2021).

40. Zhang, X., Rosenstein, B. S., Wang, Y., Lebwohl, M. & Wei, H. Identification of possible reactive oxygen species involved in ultraviolet radiation-induced oxidative DNA damage. *Free Radic. Biol. Med.* **23**, 980–985 (1997).

41. Brugè, F., Tiano, L., Cacciamani, T., Principi, F. & Littarru, G. P. Effect of UV-C mediated oxidative stress in leukemia cell lines and its relation to ubiquinone content. *BioFactors* **18**, 51–63 (2003).

42. Dogliotti, E., Fortini, P., Pascucci, B. & Parlanti, E. The mechanism of switching among multiple BER pathways. *Prog. Nucleic Acid Res. Mol. Biol.* **68**, 3–27 (2001).

43. Graham C.Walker, N. C. Review Article. *Mech. DNA Damage, Repair, Mutagen.* (2017) doi:10.1002/em.22087.

44. de Souza-Pinto, N. C. Repair of Oxidative DNA Damage. *Brenner's Encycl. Genet. Second Ed.* **35**, 142–143 (2013).

45. Sarre, A. *et al.* Structural and functional characterization of two unusual endonuclease III enzymes from Deinococcus radiodurans. *J. Struct. Biol.* **191**, 87–99 (2015).

46. Sarre, A. *et al.* The three Endonuclease III variants of Deinococcus radiodurans possess distinct and complementary DNA repair activities. *DNA Repair (Amst).* **78**, 45–59 (2019).

47. Hua, X. *et al.* Three nth homologs are all required for efficient repair of spontaneous DNA damage in Deinococcus radiodurans. *Extremophiles* **16**, 477–484 (2012).

48. Kurthkoti, K., Kumar, P., Sang, P. B. & Varshney, U. Base excision repair pathways of bacteria: New promise for an old problem. *Future Med. Chem.* **12**, 339–355 (2020).

49. Sarre, A., Ökvist, M., Klar, T., Moe, E. & Timmins, J. Expression, purification and crystallization of two endonuclease III enzymes from Deinococcus radiodurans. *Acta Crystallogr. Sect. F Struct. Biol. Commun.* **70**, 1688–1692 (2014).

50. Reon, B. J., Nguyen, K. H., Bhattacharyya, G. & Grove, A. Functional comparison of Deinococcus radiodurans Dps proteins suggests distinct in vivo roles. *Biochem. J.* **447**, 381–391 (2012).

51. Santos, S. P. *et al.* Dps from Deinococcus radiodurans: Oligomeric forms of Dps1 with distinct cellular functions and Dps2 involved in metal storage. *FEBS J.* **282**, 4307–4327 (2015).

52. Kim, S. G., Bhattacharyya, G., Grove, A. & Lee, Y. H. Crystal Structure of Dps-1, a Functionally Distinct Dps Protein from Deinococcus radiodurans. *J. Mol. Biol.* **361**, 105–114 (2006).

53. Chiancone, E. Dps proteins, an efficient detoxification and DNA protection machinery in the bacterial response to oxidative stress. *Rend. Lincei* **19**, 261–270 (2008).

54. Lim, S., Jung, J. H., Blanchard, L. & De Groot, A. Conservation and diversity of radiation and oxidative stress resistance mechanisms in Deinococcus species. *FEMS Microbiol. Rev.* **43**, 19–52 (2019).

55. Papinutto, E. *et al.* Structure of two iron-binding proteins from Bacillus anthracis. *J. Biol. Chem.* **277**, 15093–15098 (2002).

56. Santos, S. P. *et al.* SAXS Structural Studies of Dps from Deinococcus radiodurans Highlights the Conformation of the Mobile N-Terminal Extensions. *J. Mol. Biol.* **429**, 667–687 (2017).

57. Ziad Moussa, Z. M. A. J. and S. A. A. Nonenzymatic Exogenous and Endogenous Antioxidants. in *Free Radical Medicine and Biology* (2019). doi:Ziad Moussa, Zaher M.A. Judeh and Saleh A. Ahmed.

58. Bacteriol, J. & Chem, J. B. MicroCorrespondence. **29**, 381–382 (1998).

59. Ishige, K., Zhang, H. & Kornberg, A. Polyphosphate kinase (PPK2), a potent, polyphosphate-driven generator of GTP. *Proc. Natl. Acad. Sci. U. S. A.* **99**, 16684–16688 (2002).

60. Motomura, K. *et al.* A new subfamily of polyphosphate kinase 2 (Class III PPK2) catalyzes both nucleoside monophosphate phosphorylation and nucleoside diphosphate phosphorylation. *Appl. Environ. Microbiol.* **80**, 2602–2608 (2014).

61. Dai, S. *et al.* Dynamic Polyphosphate Metabolism Coordinating with Manganese Ions Defends against Oxidative Stress in the Extreme Bacterium Deinococcus radiodurans. *Appl. Environ. Microbiol.* **87**, 1–16 (2021).

62. Roberge, N. & Jia, Z. Polyphosphate Kinase 2 ( PPK2 ) Enzymes : Structure , Function , and Roles in Bacterial Physiology and Virulence. **2**, (2022).

63. Suzuki, S., Hara, R. & Kino, K. Production of aminoacyl prolines using the adenylation domain of nonribosomal peptide synthetase with class III polyphosphate kinase 2-mediated ATP regeneration. *J. Biosci. Bioeng.* **125**, 644–648 (2018).

64. Zhang, H., Ishige, K. & Kornberg, A. A polyphosphate kinase (PPK2) widely conserved in bacteria. *Proc. Natl. Acad. Sci. U. S. A.* **99**, 16678–16683 (2002).

65. Liu, Y., Chen, J. & Thygesen, A. Efficient One-Step Fusion PCR Based on Dual-Asymmetric Primers and Two-Step Annealing. *Mol. Biotechnol.* **60**, 92–99 (2018).

66. Bioinformatics. Sequence Manipulation Suite: Codon Plot.

https://www.bioinformatics.org/sms2/ (2015).

67. Hardjasa, A., Ling, M., Ma, K. & Yu, H. Investigating the Effects of DMSO on PCR Fidelity Using a Restriction Digest-Based Method. *J. Exp. Microbiol. Immunol.* **14**, 161–164 (2010).

68. QIAGEN. QIAquick Gel Extraction Kit ( 50 ) QIAquick Gel Extraction Kit ( 250 ). 2011 (2018).

69. Maurya, G. K. & Misra, H. S. Plasmids for making multiple knockouts in a radioresistant bacterium Deinococcus radiodurans. *Plasmid* **100**, 6–13 (2018).

70. NZYTech. NZYMutagenesis kit. **17**, 0–2 (2013).

71. Bolten, S. N., Rinas, U. & Scheper, T. Heparin: role in protein purification and substitution with animal-component free material. *Appl. Microbiol. Biotechnol.* **102**, 8647–8660 (2018).

72. Xiong, S., Zhang, L. & He, Q. Y. Fractionation of proteins by heparin chromatography. *Methods Mol. Biol.* **424**, 213–221 (2008).

73. Weber, P. C. Physical Principles of Protein Crystallization. *Adv. Protein Chem.* **41**, 1–36 (1991).

74. Tom Hall. Bio Edit. at https://bioedit.software.informer.com/.

75. Robert, X. and Gouet, P. Deciphering key features in protein structures with the new ENDscript server. at https://doi.org/10.1093/nar/gku316 (2014).

76. Rojkind, M., Domínguez-rosales, J., Nieto, N. & Greenwel, P. Cellular and Molecular Life Sciences Role of hydrogen peroxide and oxidative stress. *Cell. Mol. Life Sci.* **59**, 1872–1891 (2002).

77. Fisher, B. *et al.* Superoxide generated from the glutathione-mediated reduction of selenite damages the iron-sulfur cluster of chloroplastic ferredoxin. *Plant Physiol. Biochem.* **106**, 228–235 (2016).

78. Chou, F. I. & Tan, S. T. Salt-mediated multicell formation in Deinococcus radiodurans. *J. Bacteriol.* **173**, 3184–3190 (1991).

# A
# ANNEXES

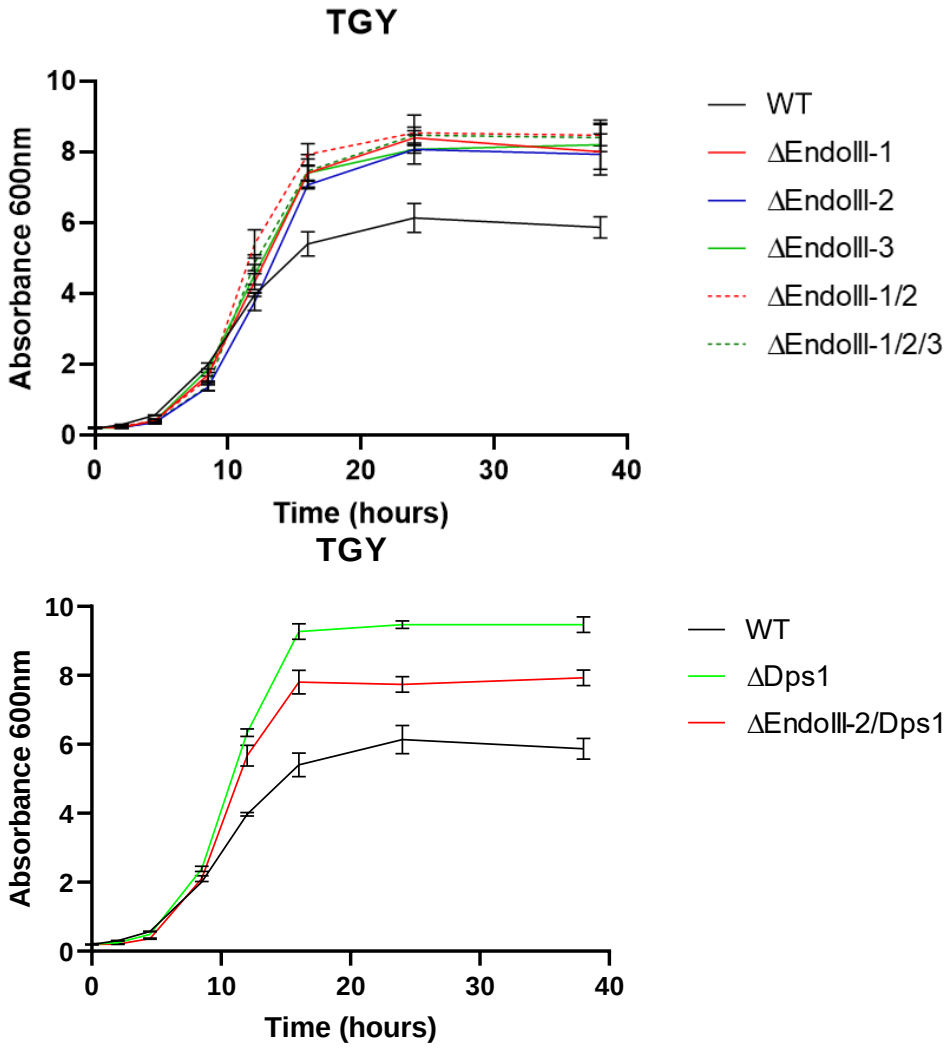


FigureA 1 Growth curves of the EndoIII and Dps1 knockout mutants constructed, in TGY.

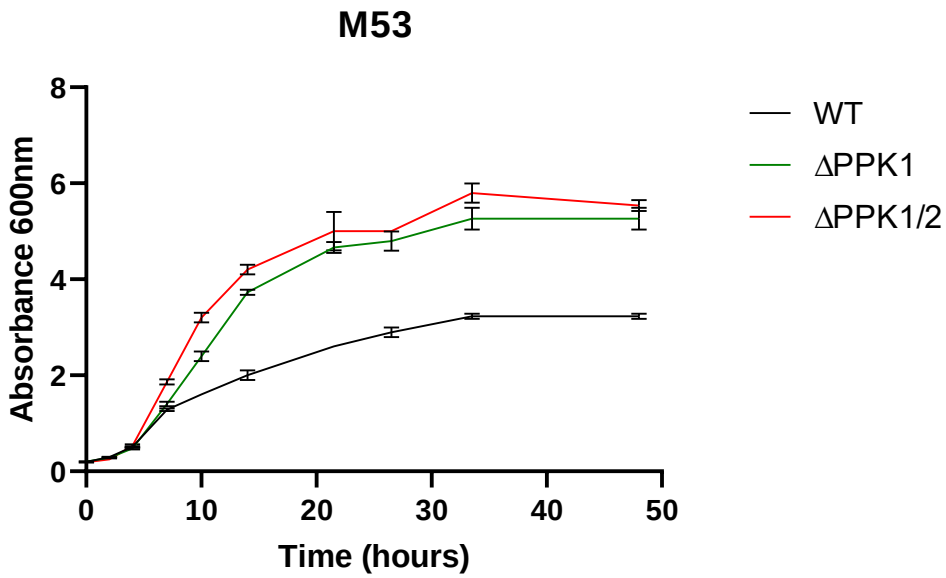


FigureA 2 Growth curves of the PPK1 and PPK1/2 knockout mutans, in M53

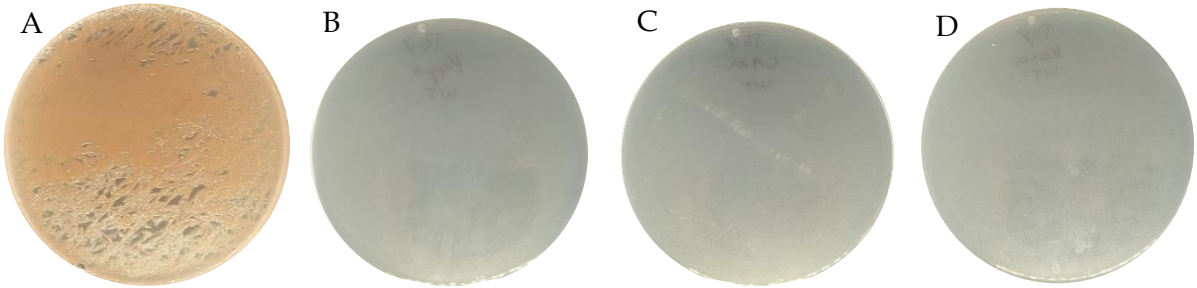


FigureA 3– Confirmation of the response of WT to the concentration of antibiotics used throughout the experiment.

A – TGY; B – TGY + Hygromycin (50µg/mL); C – TGY+Chloramphenicol (3.5µg/mL); D – TGY+Kanamycin (6µg/mL)

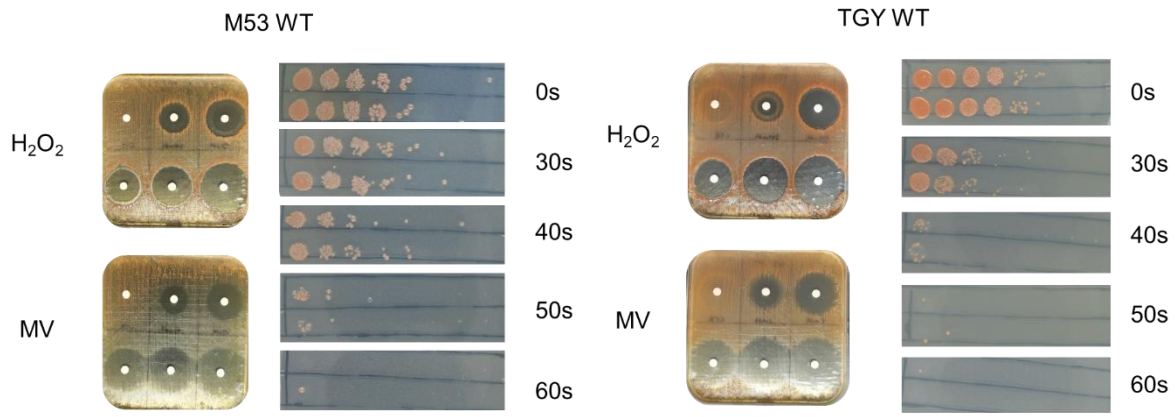


FigureA 4 Results from one of the replicates, from the oxidative stress and UV-C assays, in both media (TGY and M53) of the WT assays.

In the oxidative stress assays, triplicates were done and, in the UV-C assays, two replicates in the same plate were used as well as two plate replicates. Both types of assays had two biological replicates.

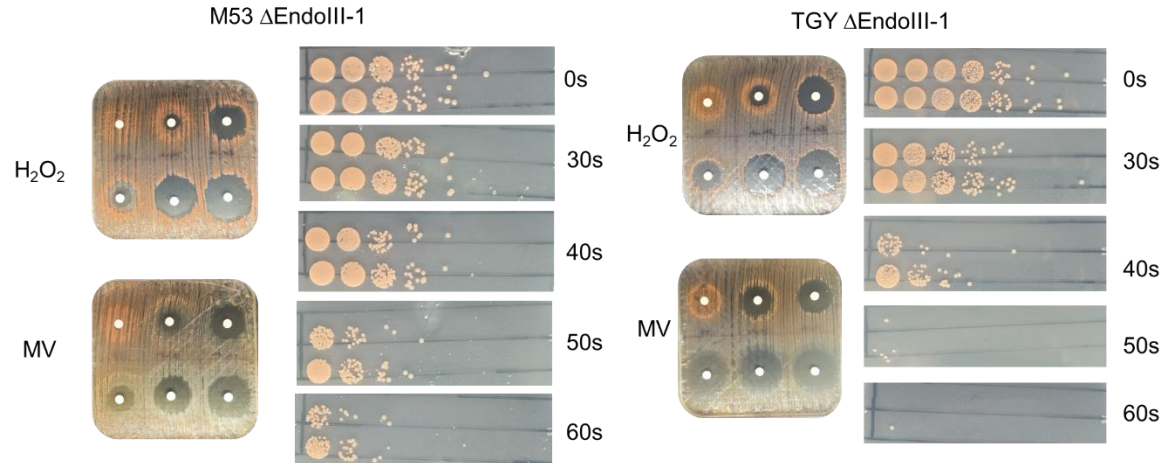


FigureA 5 Results from one of the replicates, from the oxidative stress and UV-C assays, in both media (TGY and M53) of the ΔEndoIII-1 assays.

In the oxidative stress assays, triplicates were done and, in the UV-C assays, two replicates in the same plate were used as well as two plate replicates. Both types of assays had two biological replicates.

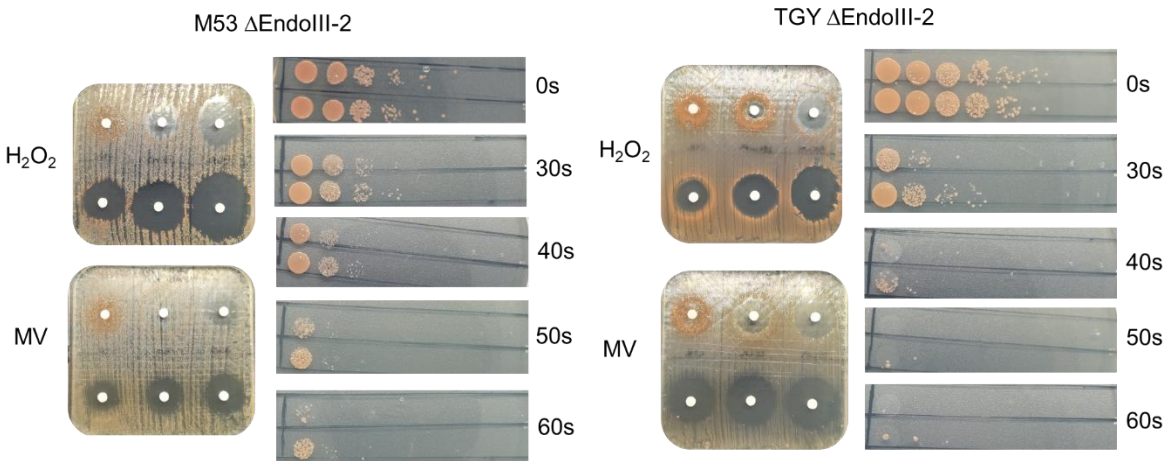


FigureA 6 Results from one of the replicates, from the oxidative stress and UV-C assays, in both media (TGY and M53) of the ΔEndoIII-2 assays.

In the oxidative stress assays, triplicates were done and, in the UV-C assays, two replicates in the same plate were used as well as two plate replicates. Both types of assays had two biological replicates.

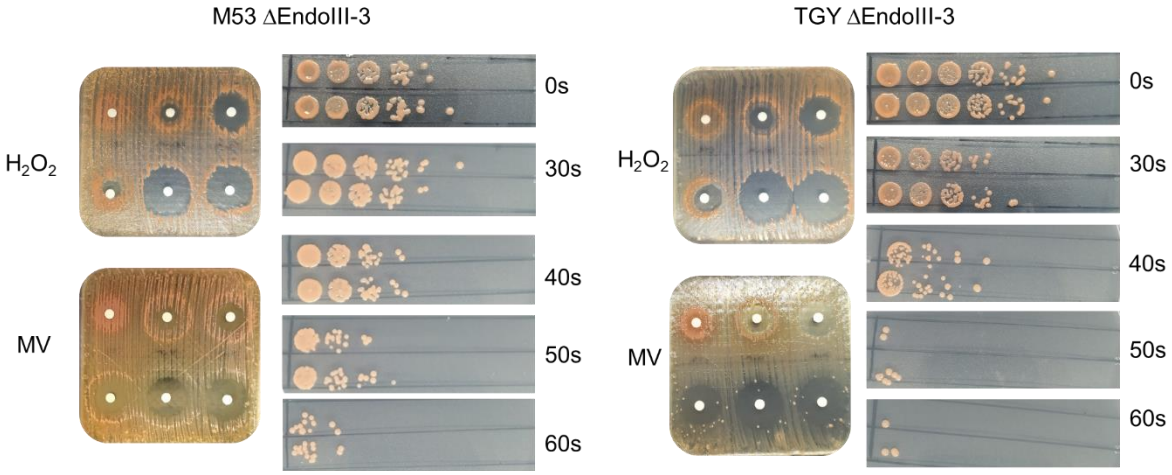


FigureA 7 Results from one of the replicates, from the oxidative stress and UV-C assays, in both media (TGY and M53) of the ΔEndoIII-3 assays.

In the oxidative stress assays, triplicates were done and, in the UV-C assays, two replicates in the same plate were used as well as two plate replicates. Both types of assays had two biological replicates.

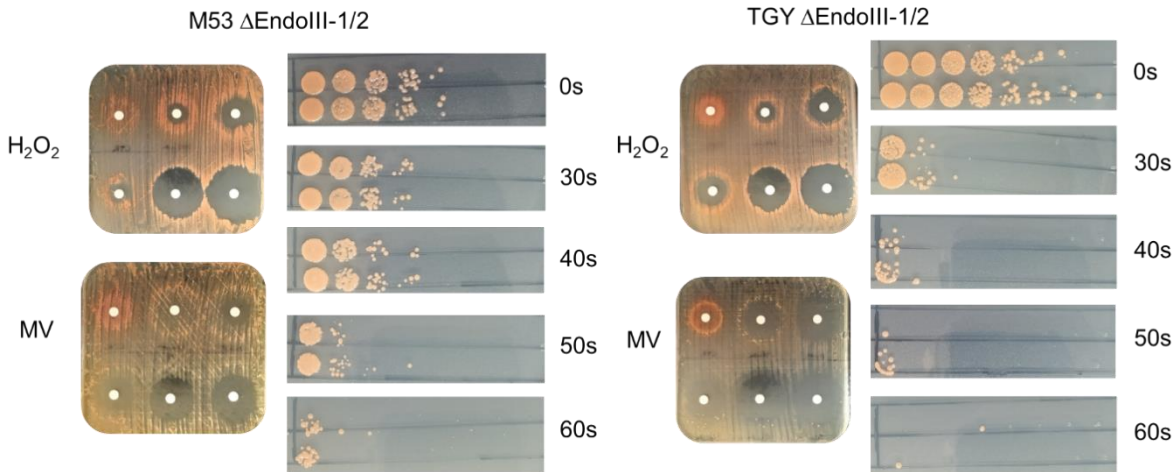


FigureA 8 Results from one of the replicates, from the oxidative stress and UV-C assays, in both media (TGY and M53) of the ΔEndoIII-1/2 assays.

In the oxidative stress assays, triplicates were done and, in the UV-C assays, two replicates in the same plate were used as well as two plate replicates. Both types of assays had two biological replicates.

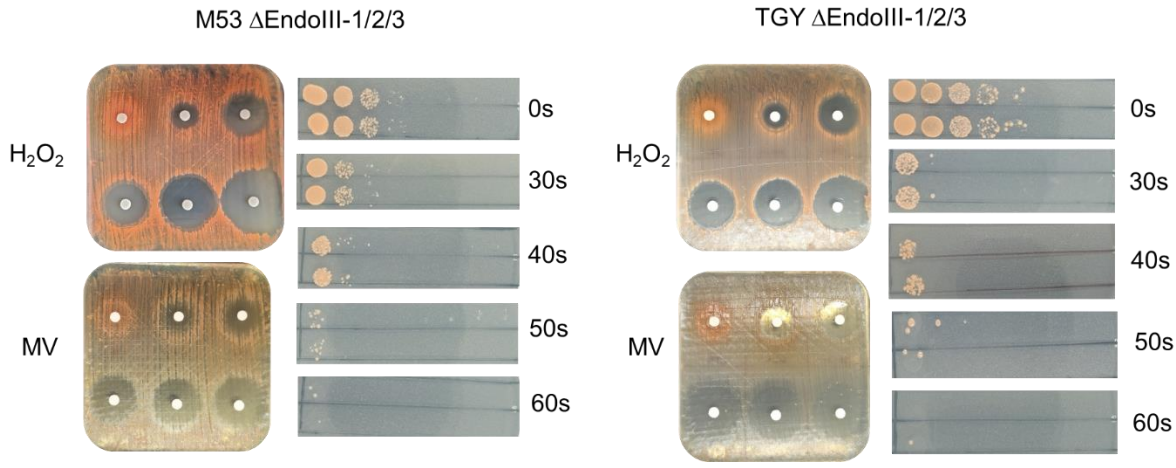


FigureA 9 Results from one of the replicates, from the oxidative stress and UV-C assays, in both media (TGY and M53) of the ΔEndoIII-1/2/3 assays.

In the oxidative stress assays, triplicates were done and, in the UV-C assays, two replicates in the same plate were used as well as two plate replicates. Both types of assays had two biological replicates.

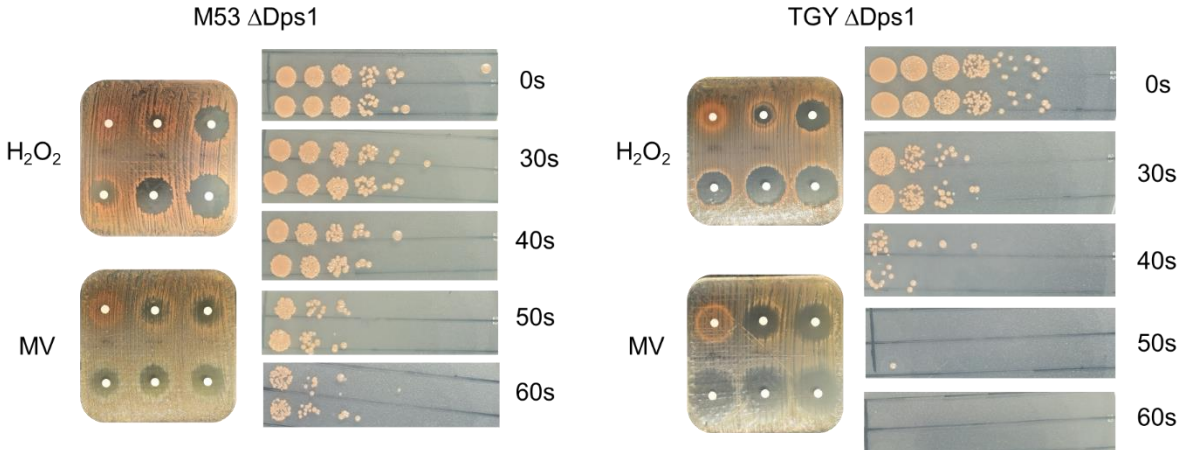


FigureA 10 Results from one of the replicates, from the oxidative stress and UV-C assays, in both media (TGY and M53) of the ΔDps1 assays.

In the oxidative stress assays, triplicates were done and, in the UV-C assays, two replicates in the same plate were used as well as two plate replicates. Both types of assays had two biological replicates.

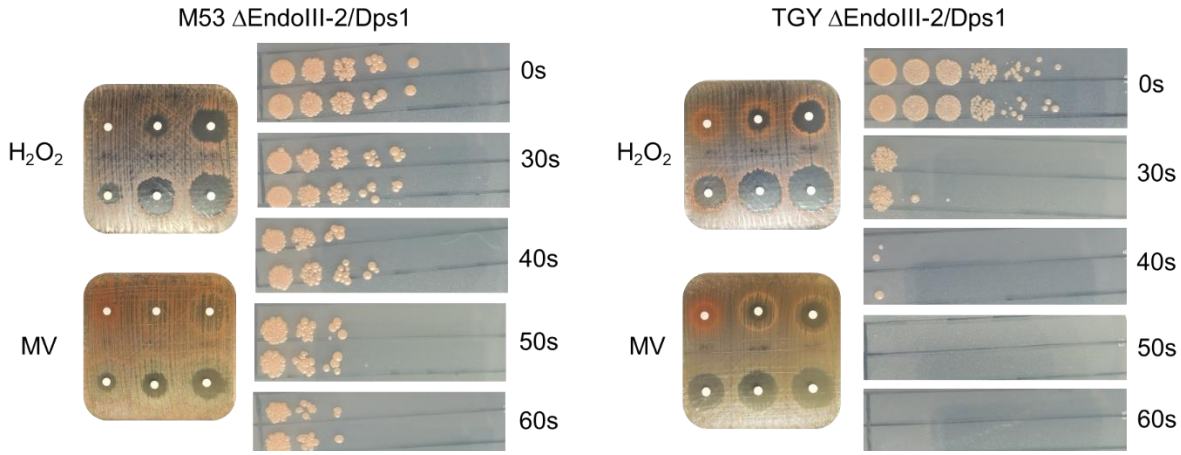


FigureA 11 Results from one of the replicates, from the oxidative stress and UV-C assays, in both media (TGY and M53) of the ΔEndoIII-2/Dps1 assays.

In the oxidative stress assays, triplicates were done and, in the UV-C assays, two replicates in the same plate were used as well as two plate replicates. Both types of assays had two biological replicates.

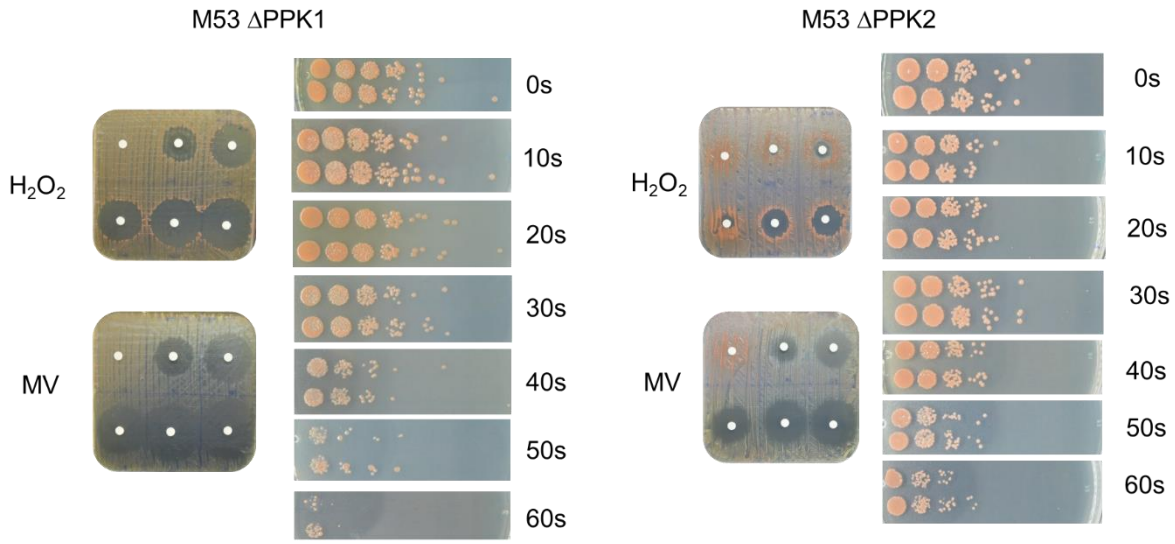


FigureA 12 Results from one of the replicates, from the oxidative stress and UV-C assays, in M53 of the ΔPPK1 and ΔPPK2 assays.

In the oxidative stress assays, triplicates were done and, in the UV-C assays, two replicates in the same plate were used as well as three plate replicates. Both types of assays had two biological replicates.

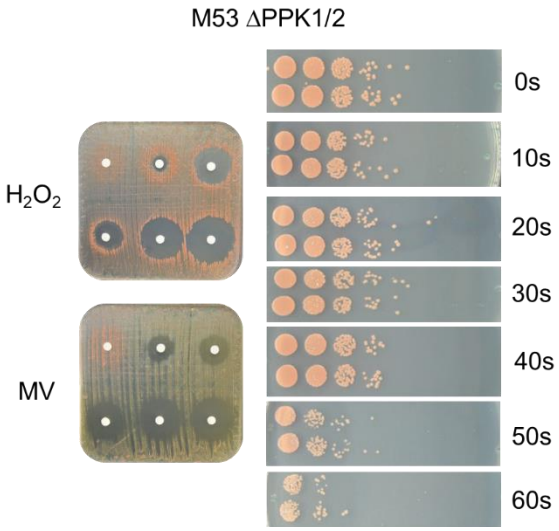


FigureA 13 Results from one of the replicates, from the oxidative stress and UV-C assays, in M53 of the ΔPPK1/2 assays.

In the oxidative stress assays, triplicates were done and, in the UV-C assays, two replicates in the same plate were used as well as three plate replicates. Both types of assays had two biological replicates.

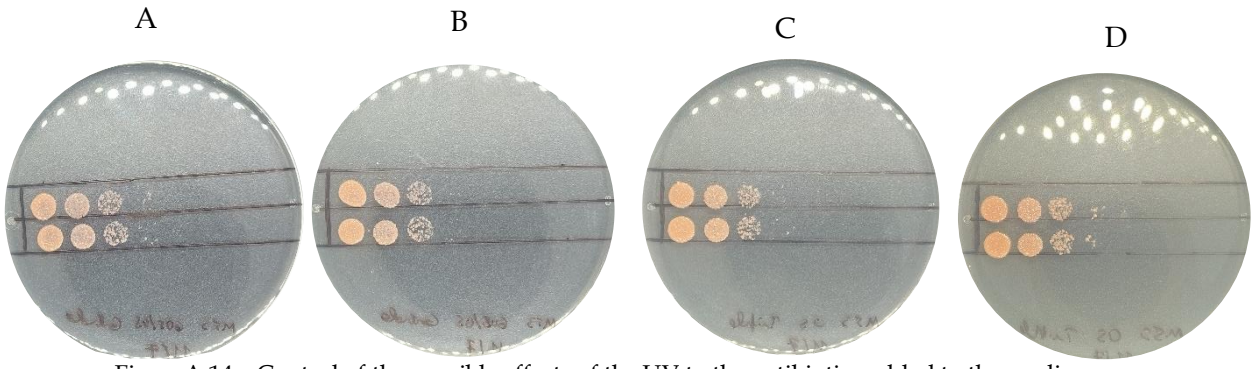


FigureA 14 – Control of the possible effects of the UV to the antibiotics added to the medium.
Plates A and B were irradiated for 60 seconds with UV-C radiation before pipetting the 5µL drops of different dilutions of the culture. Plates C and D were not exposed to UV-C radiation.

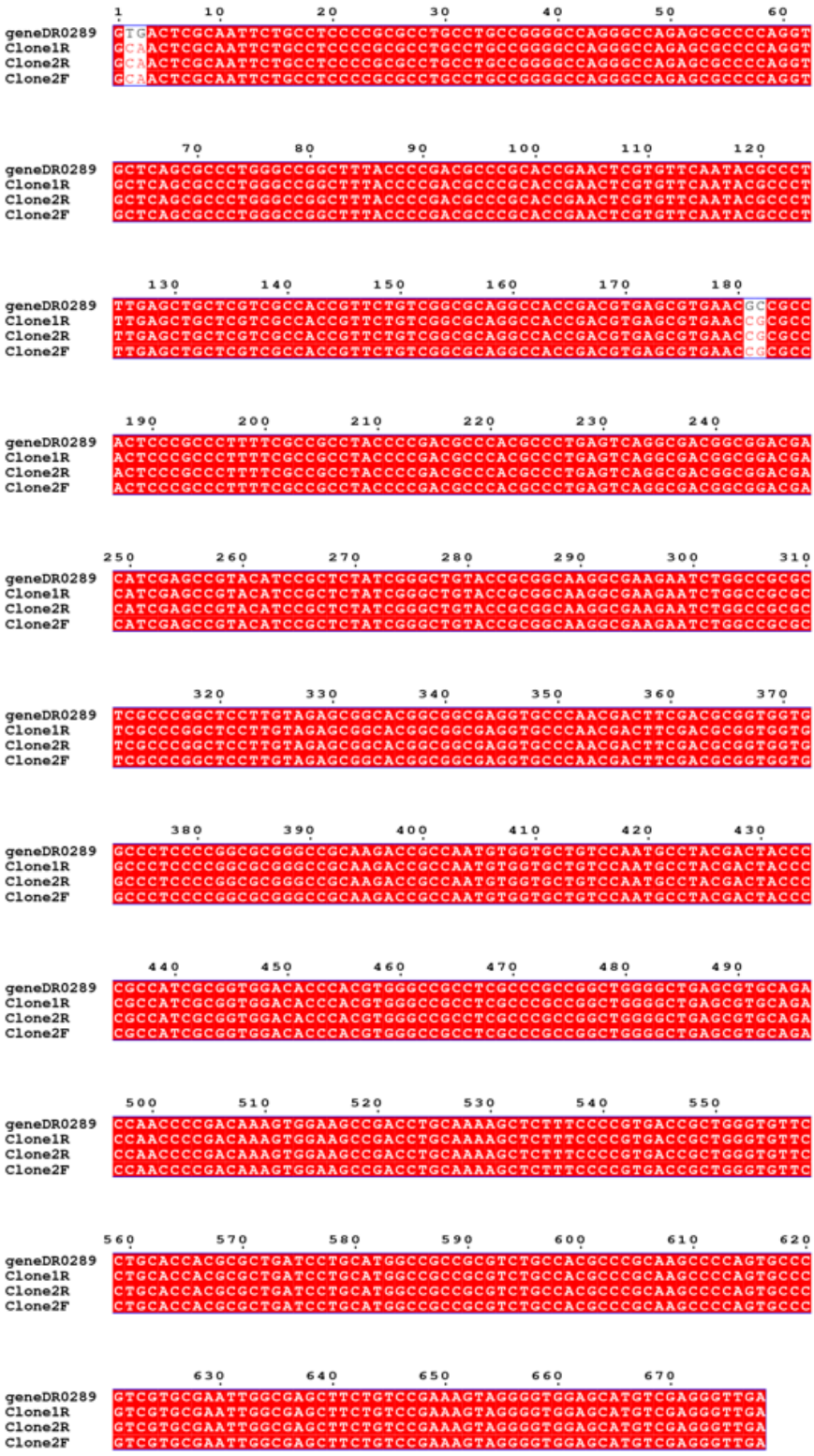


FigureA 15 – Nucleotide sequence of the EndoIII-2 gene. Mutations are highlighted in white.